Dalton Transactions

ROYAL SOCIETY OF CHEMISTRY

PERSPECTIVE

View Article Online
View Journal | View Issue

Cite this: *Dalton Trans.*, 2025, **54**, 17360

Development of nanosized materials using organosulphur compounds as building blocks for applications in catalysis and electrocatalysis

Anupma Tyagi,[a] Suraj Purohit,[a] Nivedita Kunwar,[a] Anurag Bahuguna,[a] Kamal K. Pant[b] and Arun Kumar *[a]

Received 8th August 2025,
Accepted 7th October 2025

DOI: 10.1039/d5dt01892g

rsc.li/dalton

Over the past few decades, there has been extensive utilization of organosulphur compounds for the development of nanocatalysts for various chemical reactions. A wide array of organosulphur compounds and their preformed molecular complexes with numerous metals (including palladium, cobalt, copper, lead, nickel and silver) have been used for this purpose. Such compounds, complexes and nanocatalysts can be developed using diverse techniques. This article encompasses the strategies employed in designing relevant organosulphur compounds and exploring their utility in developing catalytically active nanomaterials. Various methodologies are discussed for the synthesis of nanomaterials, such as the single source precursor (SSP) method, reduction method for colloidal synthesis and indirect generation of nanoparticles. The intricacies of different synthetic methodologies are revealed in detail in this article. Additionally, the applications of such nanocatalysts in a diverse range of chemical transformations (such as Suzuki coupling, Sonogashira coupling, Heck coupling, C–O coupling reaction, and cross-dehydrogenative coupling (CDC)) are the main focus of this article. Their use in electrochemical studies is also rationalized in the context of the reactions such as the hydrogen evolution reaction (HER), oxygen evolution reaction (OER) and overall water splitting. A critical assessment of the variations in catalytic performances and the mechanistic aspects of nanocatalysis is also included. Moreover, it sheds light on the future perspectives of this field.

1. Introduction

Nanoscience is considered one of the key technology areas of the 21st century.[1,2] It is well known that materials have unique properties at the nanoscale. Some of these properties are remarkable. The Lycurgus cup, consisting of gold and silver nanoparticles, was an early example of nanostructured materials.[3] When lit from the outside, it appeared opaque green. However, when it is lit inside, it glows red.[3] The word "nanomaterial" refers to any solid with nanometer-scale dimensions. The European Commission (EC) defined "nanomaterials" for the first time in 2011 as "a natural, incidental, or manufactured material containing particles in an unbound state or as an aggregate or as an agglomerate".[4] Nanocatalysis has been a very important field in the domain of nanoscience since a long period of time.[5]

Nanocatalysts have gained much popularity because they exhibit exceptional properties, such as selectivity,[6,7] high activity, durability, recoverability, recyclability and other unique attributes. Such properties are rarely observed in the bulk counterparts of these catalysts. Gold nanoparticles exhibit unexpected catalytic activity, which differs from that of the bulk gold. This can be taken as a good example of nanocatalysis.[8–11] Nanocatalysis is sometimes referred to as a "semiheterogeneous"[12] or "soluble heterogeneous"[13] mode of catalysis. Nanoparticles can behave as active and stable heterogeneous catalysts or support materials for various catalytic groups.[14] Hence, they also act as a bridge between homogeneous and heterogeneous catalysis.[14] Such particles have a large surface area, which enables them to be in better contact with the reactants. As far as the ease of separation from reaction mixtures is concerned, nanostructured catalysts can function as heterogeneous catalysts. Like homogeneous catalytic systems, they exhibit customisable catalytic activity and selectivity at the nanoscale.[15,16] It is worth noting that nanocatalysts with superior activity, stability, and selectivity[6,7] can be developed and synthesised simply by controlling their sizes, shapes, and morphologies.[14,17]

Nanocatalysis is also referred to as a tool to promote green chemistry, *i.e.*, a philosophy that promotes sustainable principles for reducing or eliminating chemicals and chemical processes that may create harm to the environment. It is primarily

[a]*Department of Chemistry, School of Physical Sciences, Doon University, Dehradun-248012, India. E-mail: arunkaushik@gmail.com, akumar.ch@doonuniversity.ac.in*
[b]*Department of Chemical Engineering, IIT Delhi, New Delhi-110016, India*

guided by twelve key concepts given by Paul Anastas and John Warner. Catalysis is one of the most significant principles in green chemistry. High-performance catalysts may open the door to green chemistry. For example, the use of metals (catalysts) in low quantities for performing the reactions successfully may result in considerable cost savings in chemical processes. This objective may be achieved using green and sustainable catalysts with high activity, improved selectivity, hassle-free recovery from the reaction media, durability or stability, recyclability, and low-cost. The majority of these critical challenges might be addressed using nano-sized metal particles as catalysts. As a result, catalysis by metals at the nanoscale is also a tool to enhance the sustainability of chemical processes. If such catalysts are highly active, the requirement and use of extreme reaction conditions may be avoided, resulting in energy-efficient processes. The increase in the selectivity of such catalysts reduces the formation of the by-products and allows chemical reactions to occur in a specific manner with low consumption of the substances, *i.e.*, reactants. Through the enhancement in atomic efficiency and waste avoidance, the increase in the recyclability of catalytically active nanomaterials may also promote green chemistry.[18]

Organosulphur compounds are very significant in the context of the development of all kinds of catalysts, including homogeneous, heterogeneous and nanocatalysts.[19,20] Such compounds have sulphur covalently bonded with carbon in the framework of the organic molecules. Sulphur is an element identified in 1777 by the French chemist Antonie Lavoisier (1743–1794).[21] It exhibits an electron donation ability and shares similarities with non-metals (like selenium) of the same group of the periodic table. However, many of its properties (such as high electronegativity, smaller size, high electron affinity, and non-metallic character) are different from those of selenium. A large variety of organosulphur compounds have been designed and explored for the development of a wide range of catalysts and electrocatalysts. Such compounds are extensively used in various forms, such as thioethers, thiols, thiosemicarbazones, thiourea, Schiff bases, sulphur-containing N-heterocyclic carbenes (NHCs), and sulphur-containing pincer ligands. These compounds behave as versatile ligands and play a crucial role in the development of diverse nanocatalytic systems. A few reviews have been published in the area of nanocatalysis. However, an analysis of recent developments in the field of the role of organosulphur compounds in the field of catalysis and electrocatalysis has rarely been focused on.

This article comprehensively delves into the advancements related to the synthesis and utilization of organosulphur compounds in the development of nano-catalytic systems. It extensively covers various types of chemical transformations carried

Anupma Tyagi

Anupma Tyagi is a DST-INSPIRE fellow and a PhD scholar under the supervision of Dr Arun Kumar in the Department of Chemistry, Doon University, Dehradun (Uttarakhand, India). She was born in 1997 in Roorkee, Uttarakhand (India). She was a student in the Department of Chemistry, Doon University, Dehradun (India) from 2015 to 2020. She earned a gold medal for securing first rank in her MSc at Doon University. She carried out her dissertation under the supervision of Dr Arun Kumar (Department of Chemistry) at Doon University in the area of the development of tellurium ligated ligands and complexes for catalysis. The Department of Science and Technology (Ministry of Science and Technology, Government of India) awarded her a highly prestigious, highly competitive and national-level DST-INSPIRE fellowship for 05 years for pursuing a PhD. Currently, she is working on the development of metal sulphide-, selenide-, telluride- and phosphide-based nanomaterials and their applications in various organic transformation reactions, such as Sonogashira coupling, Suzuki coupling, aldehyde to amide transformation, C–H activation, transfer hydrogenation reactions, and in electrocatalysis, such as the HER and OER.

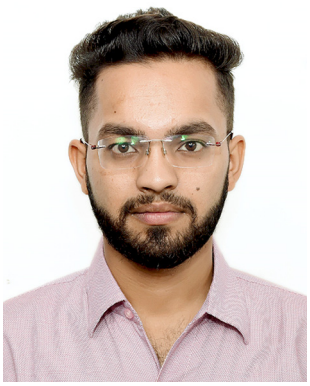

Suraj Purohit

Suraj Purohit is a DST-INSPIRE fellow and a PhD scholar under the supervision of Dr Arun Kumar in the Department of Chemistry at Doon University, Dehradun (Uttarakhand, India). He was born in 1998 in Chamoli, Uttarakhand (India). He completed his BSc from Hemvati Nandan Bahuguna Garhwal (Central) University in 2018. He completed his MSc degree at Sri Dev Suman Uttarakhand University in 2020 and earned a gold medal for securing the first rank in the university during his MSc. He also qualified the national-level exam GATE-2022 with AIR 1287 and the joint CSIR-UGC NET (AIR 48). He joined the Department of Chemistry, Doon University, Dehradun, as a PhD research scholar in 2021. The Department of Science and Technology (Ministry of Science and Technology, Government of India) awarded him with the highly prestigious, highly competitive and national-level DST-INSPIRE fellowship for 05 years for pursuing a Ph.D. Currently, he is working on the development of palladium phosphide- and palladium telluride-based nanomaterials and their applications in various organic transformation reactions, like Suzuki coupling, C–O coupling, aldehyde to amide conversion, transfer hydrogenation, and electrocatalysis.

out using such nanocatalysts, including Suzuki–Miyaura coupling, Heck coupling, Sonogashira coupling, C–O coupling, and cross-dehydrogenative coupling (CDC). An in-depth analysis of the electrochemical applications of these nanocatalysts for the hydrogen evolution reaction (HER), oxygen evolution reaction (OER), and overall water splitting is also included. Additionally, this article critically evaluates the diversity in the catalytic potential, recyclability, and mechanistic aspects of catalysis. It also includes a comparative analysis focusing on the efficiency and other advantages of this unique class of catalysts.

2. Roles of ligands and preformed metal complexes in the development of nanocatalytic systems

In the case of homogeneous catalysts, the role and function of the ligands is quite clear in determining and rationalizing the activity, selectivity and efficiency of catalytically active molecular complexes. However, the same is not true in the case of nanocatalysts and heterogeneous catalysts. It is assumed that the ligands play multiple roles in metal-based nanocatalytic systems.[22] Stabilization of the particles in the nano-size range is one of them. Other roles are yet to be studied thoroughly and established fully. As far as the role in stabilization is concerned, it is well-established that a stabilizing ligand primarily functions to prevent agglomeration, which is a tendency of the nanoscale materials. Hence, the stabilizing ligand renders them catalytically active and makes them suitable for applications in catalysis. It is unambiguous that dispersion of stabilized NPs, their catalytic performance (*i.e.*, the outcome or consequence of their activity and efficiency), composition, solubility, morphology, recyclability and size are affected by the stabilizing ligand or capping agents up to a small or significant extent.[23] The interaction between metal nanoparticles and stabilizing agent may be a strong covalent linkage, or chemisorption, or electrostatic in nature. The possibility of Ostwald ripening becomes low when the ligand adheres tightly to the metal surface. When the binding is very much strong, the circumstances are not favourable for the molecules that are approaching the surface of the nanoparticles. Such a condition can undermine catalytic activity by competing with substrate binding.[24] Hence, for optimized catalytic activity and stability of the catalytic system, proper binding strength of the stabilizing ligand is crucial.[23,24] The adoption of the reaction pathway and the coordination sphere of the metal is also manipulated by metal–ligand interaction and steric repulsions. The nature of the stabilizing ligand also affects the stability of nanocatalysts. It is also rationalized that two different interfaces are in existence due to a capping agent-generated organic shell on the nanoparticle surface (*i.e.* the metal–ligand interface and the ligand–solution interface).[23] If the capping agent is not suitable, it can act as a "poison" for the nanocatalyst and limit the availability of the active sites.[25] Hence, several studies have been performed on "ligand-free" synthesis of noble metal-based nanocatalytic systems.[26] Nonetheless, due to the numerous benefits, such as controlling the size and the facet of nanoparticles during nanoparticle synthesis, ligands are utilized as building blocks for the development of nanocatalysts. Most of the efforts to date have been limited to exploring the role of molecular ligands in controlling the size and facet of nanoparticles during nanoparticle synthesis.[22] Stabilizers such as dendrimers, surfactants, polymers, ionic liquids, and organofluorous ligands are used for the development of nanocatalysts.[27,28] Many times, they completely encapsulate the nanoparticles, rendering them catalytically inactive. Therefore, organic ligands, such as thiols, have been found to be stabilizers. In some cases, such compounds lead to the formation of larger aggregates, and the depression in catalytic efficiency is negligible.[29]

Organosulphur compounds have a strong coordinating site due to which they can bond with transition metals very well.

Nivedita Kunwar

Nivedita Kunwar was born in 2001 in Vikasnagar, Dehradun, Uttarakhand. She completed her integrated MSc in Chemistry at Doon University, where she actively participated in research under the supervision of Dr Arun Kumar. Her work focuses on nanoparticles and catalysis, through which she has developed expertise in organic synthesis, nanoparticle fabrication, and C–C coupling reactions.

Anurag Bahuguna

Anurag Bahuguna, a PhD scholar at the University of Bath (UK) at present, was born in Roorkee, Uttarakhand, in 2001. He completed his school education in 2018 in Rishikesh, Uttarakhand (India). He joined the Department of Chemistry, Doon University, Dehradun, as an undergraduate student in 2018 and has recently completed his master's programme there. During his time at Doon University, he worked in the research group under the supervision of Dr Arun Kumar, with research interests in the catalysis of coupling reactions, nanomaterials and organic/inorganic synthesis.

Thus, they act as highly efficient stabilizers for metal nanoparticles.[24] They have been utilized for designing nanocatalysts (Chart 1) using three approaches. One is the formation of NPs through the preformed molecular complexes, which provide high and uniform dispersion of the catalytically active nanocatalytic species.[30] The other approach is to use them as stabilizers for transition metal nanoparticles due to the excellent affinity of S donor groups with transition metals. The third approach is through the isolation and separation of *in situ*-generated nanoparticles during chemical transformations. These particles not only exhibit long term stability in solution and good catalytic activity but also provide anti fouling and responsive properties for many biomedical and catalytic applications.[24,31,32] Such sulphur containing compounds have also been reported to lead to the development of the catalytic systems, which play a central role in forming selective products. In such cases, their asymmetric nature leads to the formation of optically active products.[33]

Unlike the nanocatalysts, the preformed metal complexes have a definite and more specified role for the ligands in the context of catalytic activity.[34] The nature and structure of the coordination sphere around the metal are completely determined by the ligand molecule(s). Thus, they play a significant controlling role on the activity and reactivity of the metal complexes in catalysis. The local ligand-induced microenvironment allows the molecular complex to grant permission or impose a restriction on the substrate molecules during their movement to reach the catalytically active metal site. This is how the ligand molecules play an important role in regulating the kinetic reactivity of the metal complex, leading to narrowing down or broadening the substrate scope for a specific reaction.[34] The efficiency of the catalyst also relies on the lability of the bond between the metal and donor atom. In addition to activity and efficiency, ligands also affect the solubility of metal complexes in different solvents.[36] As a result, ligand design has garnered significant attention from research groups worldwide.[35]

During the past two decades, the preformed metal complexes (Chart 2) have also been utilized to design tailor-made nanocatalytic systems for various catalytic and electrochemical applications. Such complexes have been used as single source precursors (SSPs) for synthesizing nanocatalytic systems or they have been used to carry out the *in situ* generation of the nanoparticles during catalysis.

3. Methodologies utilized for developing nanocatalytic systems using organosulphur-based ligands and metal complexes

Nanocatalytic systems (Charts 3–5) have been studied extensively in terms of their development and characterization

Kamal K. Pant

Prof. Kamal Kishore Pant received his PhD (Chemical Engineering) degree from the Indian Institute of Technology Kanpur in 1997. He took over as the director of the Indian Institute of Technology Roorkee in 2022. Prof. Pant is a Full Professor at IIT Delhi and held the positions of Petrotech Chair and Federation of Indian Petroleum Industries (FIPI) Chair Professor, Chairman of GATE and JAM, Chairman of the Library, Head of the Department of Chemical Engineering, and Dean Faculty at the Indian Institute of Technology Delhi. He is an Adjunct Faculty at the University of Saskatchewan in Canada. He is also a fellow of several national and international academies, which include the National Academy of Sciences India (NASI) and the Indian National Academy of Engineering (INAE). Prof. Pant has published more than 300 research papers in journals of high repute with more than 21000 citations and guided 50 PhD scholars. His area of interest is futuristic technologies of national and international importance, e.g., Green catalysis, hydrocarbon conversion processes, biomass conversion and biofuel production, CO_2 conversion technologies, e-waste and plastic waste management.

Arun Kumar

Dr Arun Kumar is a fellow of the Royal Society of Chemistry (FRSC), United Kingdom. He is a native of Ghaziabad (India) and studied at IIT Delhi (2003–2009) for his PhD under the supervision of Prof. A. K. Singh. He has been a recipient of various fellowships (viz. JRF, SRF, RA and SRA) from the CSIR India. After joining Doon University, Dehradun, in July 2015, he served as the founding Head of the Chemistry Department and member of the Academic Council and Court of Doon University. He was also appointed as the Director, Research and Development Cell, Doon University in February 2021. In addition to completing some research projects (funded by SERB and UGC), he has contributed to publishing more than six dozen of articles in international journals of high repute, and 08 book chapters. His h-index is >35, and his i-10 index is >50. Currently, his research group is working on the development of new catalysts and materials for challenging organic transformations.

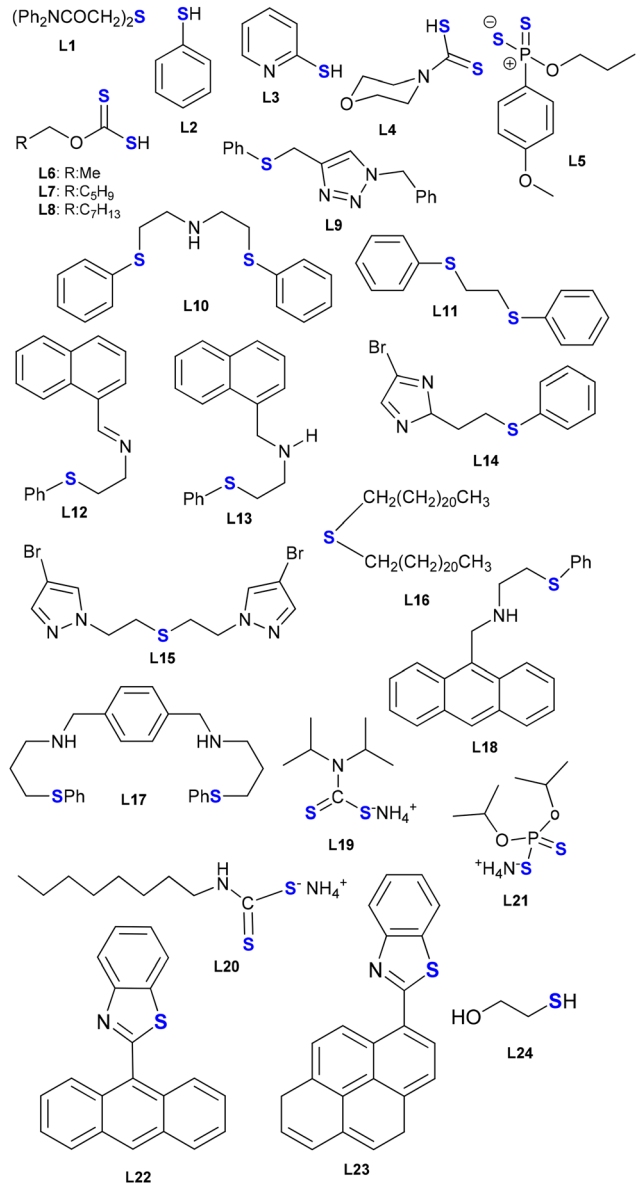

Chart 1 Organosulphur ligands **L1–L24** used in the development of nanocatalytic systems.

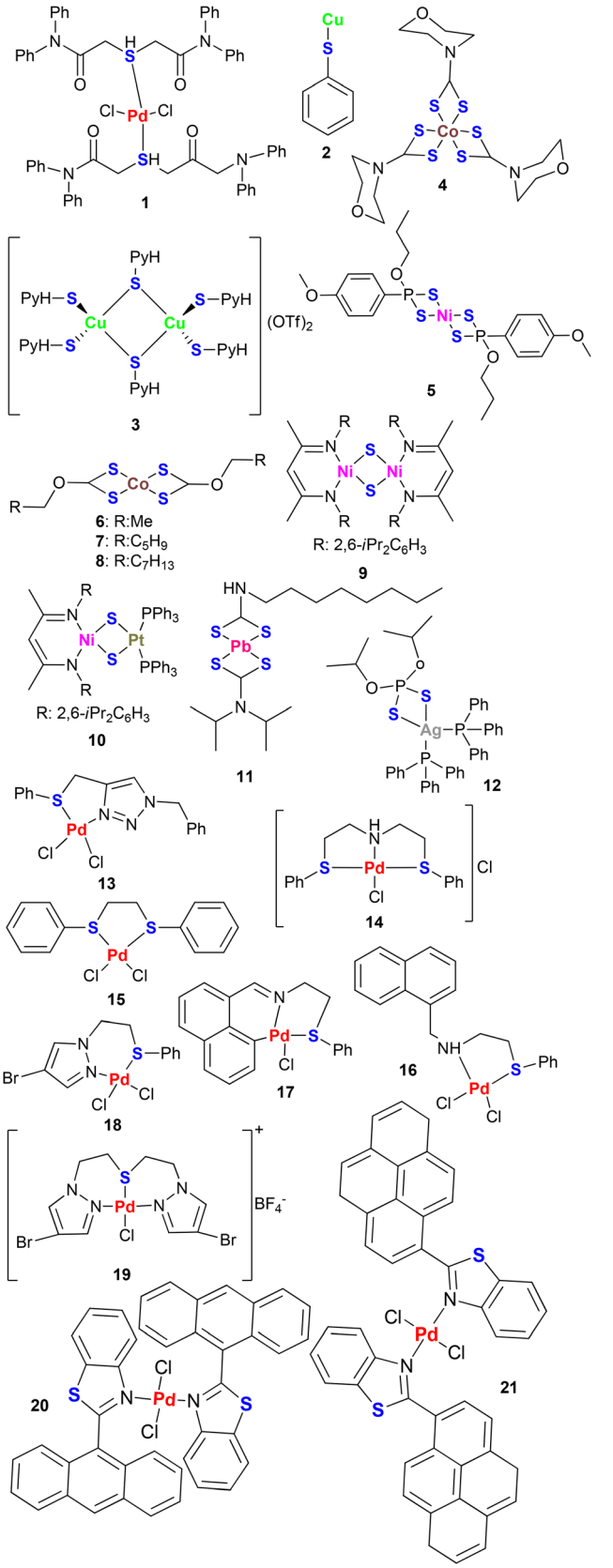

Chart 2 Organosulphur-ligated complexes **1–21** utilized for the development of nanocatalytic systems.

before being used in catalysis or electrocatalysis. In the development of such systems, organosulphur compounds have been utilized in three ways. The use of different techniques and strategies can be exercised only after a thorough investigation and understanding of the capabilities of organosulphur compounds in designing nanocatalytic systems for improved catalytic performance.

3.1. Single source precursor (SSP) method: use of organosulphur compounds as building blocks for single source molecular precursors

In this method, preformed metal complexes of organosulphur compounds are used as single source precursors for developing catalytically active and stable (Chart 3) metal sulphides.

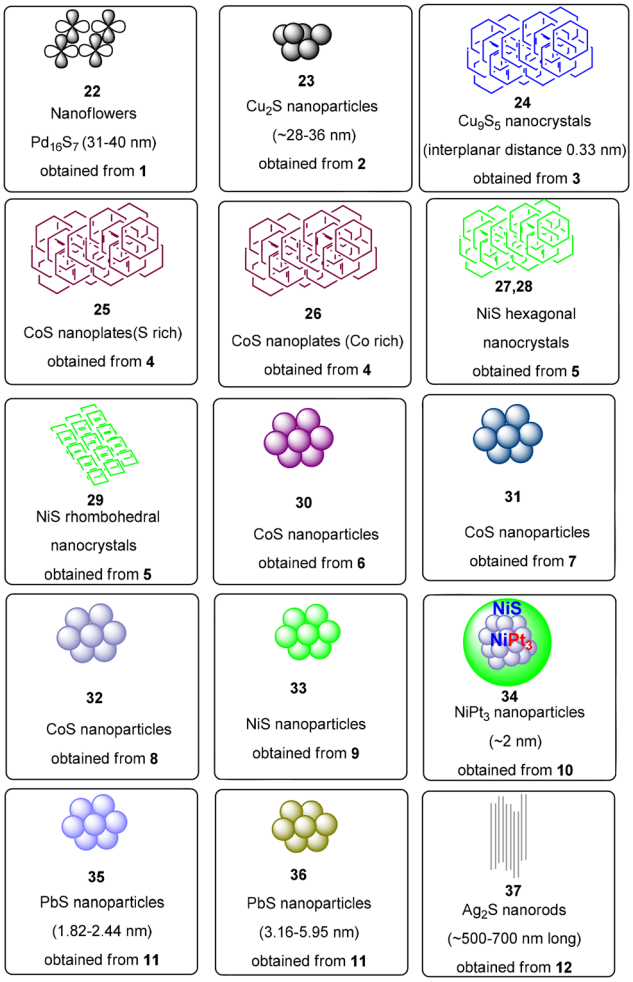

Chart 3 Nanocatalytic systems **22–37** developed using the SSP (single source precursor) method.

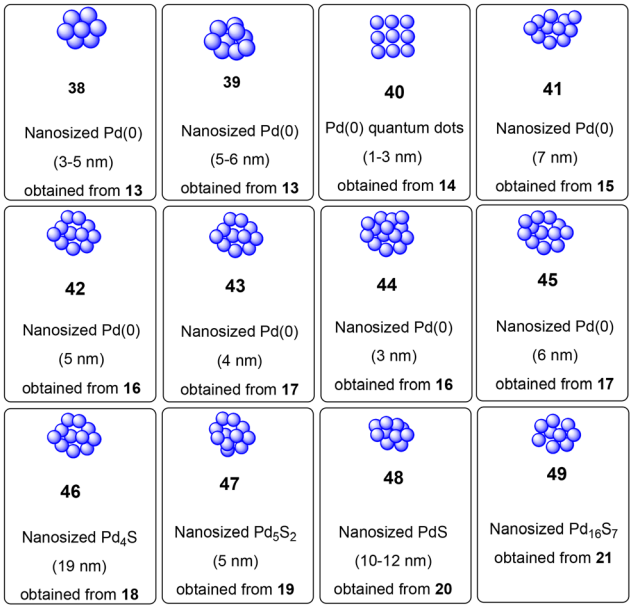

Chart 4 Nanoparticles **38–49** obtained as by-products during coupling reactions.

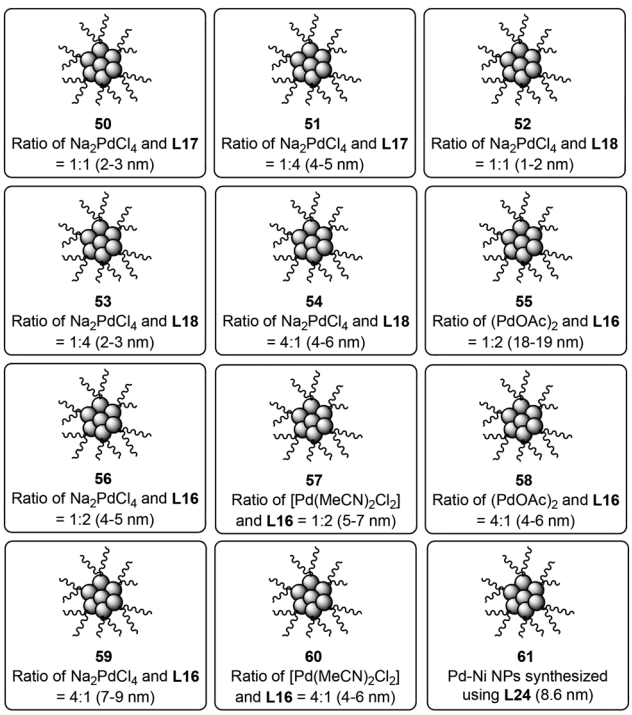

Chart 5 Nanocatalytic systems **50–61** developed using a reduction method.

The main advantage of this method is the ease with which it leads to the synthesis of the product (*i.e.*, nanomaterial). Such an ease includes the occurrence of the reaction at a moderate temperature and a straightforward protocol.

Additional advantages are the purity of nanostructures, reduction in toxicity risks and negligible issues related to air and moisture sensitivity.

Flower-shaped nanocatalyst **22** (*i.e.*, $Pd_{16}S_7$) has been synthesized by the thermolysis route (Scheme 1). In the first step, ligand **L1** reacts with the palladium precursor Na_2PdCl_4 to obtain metal complex **1**. Thereafter, nanosized $Pd_{16}S_7$ is synthesized by the thermolysis of complex **1** in trioctylphosphine (TOP) at 280 °C. The size of this nanocatalyst (Fig. 1) is nearly 31–40 nm.[37]

Nanocatalyst **23** (*i.e.*, Cu_2S) has been developed using the SSP method. Complex **2** is subjected to thermolysis (Scheme 2) at 320 °C to obtain this catalyst. The size of the nanoparticles (Fig. 2) is in the range of 28–36 nm.[38]

Nanocatalytic system **24** (*i.e.*, Cu_9S_5) has been developed using a similar method in which copper complex **3** is used as a single source precursor.[39] This complex is synthesized (Scheme 3) by reacting $Cu(OTf)_2$ and 2-mercaptopyridine thiol in DCM for 8 hours under an inert atmosphere. When this complex is subjected to thermolysis in oleylamine at 250 °C, it leads to the generation of Cu_9S_5 hexagonal nanocrystals (**24**).

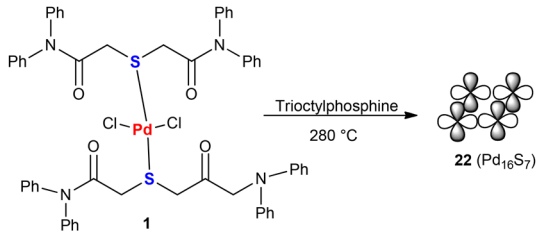

Scheme 1 Development of the flower-shaped $Pd_{16}S_7$ nanocatalyst **22** using metal complex **1** as a single source precursor.[37]

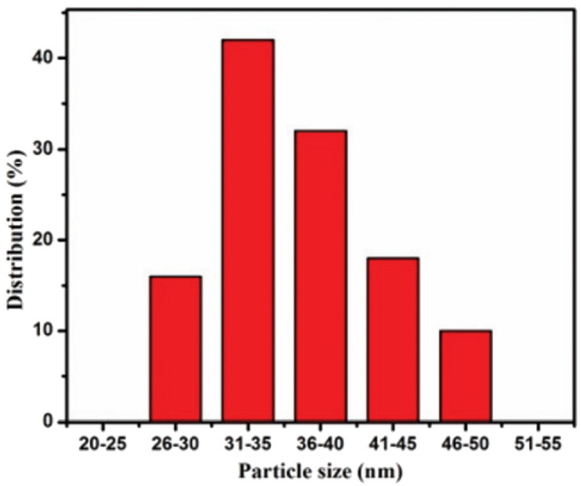

Fig. 1 Size distribution of the $Pd_{16}S_7$ nanocatalyst **22**. Reproduced from ref. 37 with permission from the Royal Society of Chemistry. Copyright {2017}.

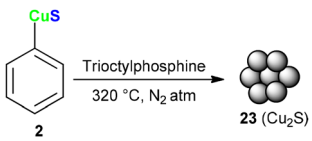

Scheme 2 Development of nanocatalyst **23** using metal complex **2** as a single source precursor.[38]

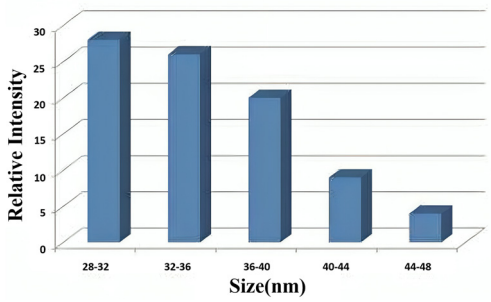

Fig. 2 Size distribution of the Cu_2S nanocatalyst **23**. Reprinted (adapted) with permission from ref. 38. Copyright {2018}, the American Chemical Society.

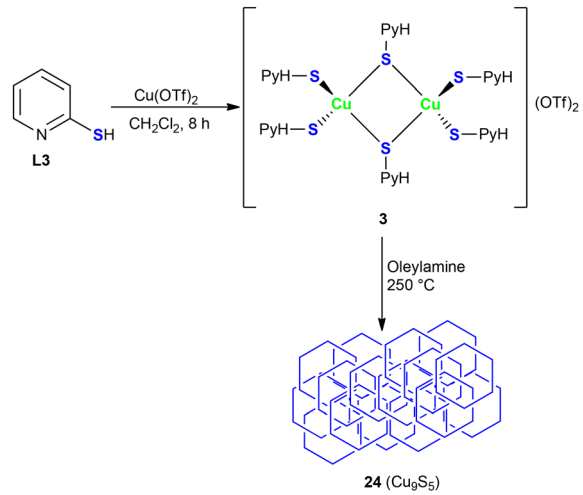

Scheme 3 Synthesis of the dinuclear copper(I) complex **3** and its use as a single source precursor to generate the nanoparticle **24**.[39]

The HR-TEM data clearly indicate that the $d(101)$ lattice fringes have an interplanar distance of 0.33 nm. This confirms the purity of the nanocatalyst.[39]

Nanocatalyst **25** is CoS (sulphur rich). It is made up of nanoplates that have a slightly sulphur-rich composition. Similarly, nanocatalyst **26** is CoS (cobalt rich). In this case, the nanoplates have a cobalt-rich composition. Both of them are obtained when cobalt complex **4** is thermolyzed (Scheme 4) in oleylamine (OLA). Temperature influences the final product in this case. When the process of thermolysis is carried out at 200 °C, the formation of the **25** (sulphur rich CoS) occurs. When the thermolysis is performed at 260 °C, **26** (cobalt rich CoS) is obtained (Scheme 4). P-XRD and XPS investigations

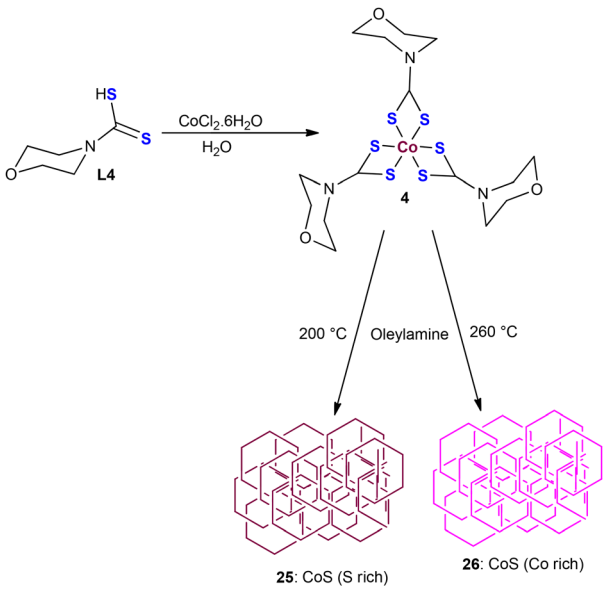

Scheme 4 Synthesis of the cobalt sulphide nanoplates **25** and **26**.[40]

provide sufficient data to confirm the successful formation of both the nanocatalysts.[40]

Nanocatalytic systems **27**, **28**, and **29** have NiS (nickel sulphide).[41] They have been synthesized using a sulphur ligated complex of nickel (*i.e.*, the **5**). Thermal degradation of this complex is carried out to obtain them. When thermolysis is carried out (Scheme 5) in the mixture of *n*-hexadecylamine and 1-octadecene system at 300 °C, hexagonal nanocrystals **27** are obtained. Interestingly, when a single molecular precursor (*i.e.*, complex **5**) is thermolyzed at 400 °C under nitrogen atmosphere and solvent free conditions, it yields hexagonal nanocrystals of **28** (Scheme 5). However, when the complex is thermolyzed at 300 °C in tri-octylphosphine oxide and ODE, rhombohedral nanocrystals of NiS (**29**) are obtained. P-XRD data are sufficient to indicate that these crystals contain NiS.[41]

Nanocatalytic systems **30**, **31** and **32** are self-capped nanoparticles of CoS (cobalt sulphide).[42] They are synthesized (Scheme 6) by the thermal decomposition of cobalt xanthate complexes **6**, **7**, and **8**, respectively. The thermolytic process is carried out at 250 °C under solvent free conditions (Scheme 6). The composition and morphology of the synthesized systems are verified using P-XRD, XPS, SEM and TEM analyses.[42] The TEM data reveal that nanoparticles **30**, **31** and **32** are spherical in shape. The size of the nanoparticles decreases with the increase in alkyl chain length; this could be due to the possibility of better dispersion of nanoparticles with longer alkyl chains. The order of the size of the nanoparticles is **30** > **31** > **32**.[42]

Moreover, **33** and **34** are interesting nanocatalytic systems.[43] Both of them contain nickel sulphide (NiS). Nanocatalyst **34** is a core–shell bimetallic alloy system. It has a nickel–platinum alloy ($NiPt_3$) protected by amorphous NiS structures (Scheme 7). Additionally, **33** is synthesized (Scheme 7) by the thermolysis of complex **9** under N_2 atmosphere at 200 °C. Interestingly, the development of **34** involves the thermolysis of a hetero-bimetallic complex of nickel and platinum (*i.e.*, complex **10**) under similar conditions.[43] The Ni–Pt nanoparticles, *i.e.*, **34**, are approximately 2 nm in size. The EDX data revealed that the compositions of Ni, Pt and S in the nanoparticles are 40%, 30% and 30%, respectively.[43]

Nanocatalytic systems **35** and **36** are the nanoparticles of PbS.[44] Nanocatalytic system **35** is developed (Scheme 8) by dissolving complex **11** (the Pb complex of an organosulphur compound) in oleic acid and thereafter infusing the same into hexadecylamine (HDA) at 360 °C for 1 hour. Similarly, nanocatalytic system **36** is synthesized (Scheme 8) using a thermogravimetric analyzer (TGA), in which complex **11** is placed in an alumina pan and the temperature is gradually increased from 30–900 °C with a continuous flow of nitrogen, yielding nanoparticles **36**.[44] Nanoparticles **35** and **36** are spherical in shape. The nanoparticles synthesized using a solvent (oleic acid and HDA), *i.e.*, **35**, are smaller in size (1.82–2.44 nm) in

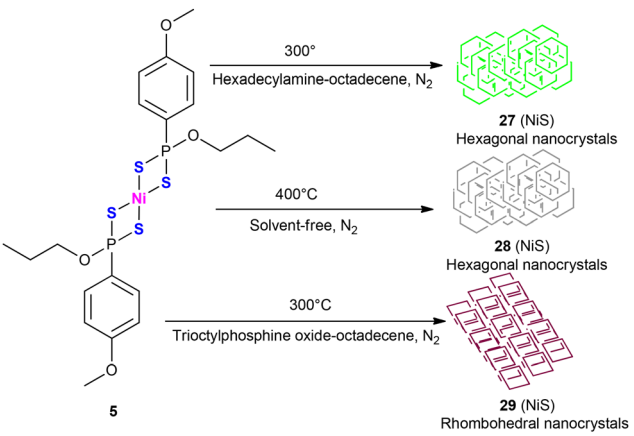

Scheme 5 Synthesis of the nanocatalytic systems **27–29**.[41]

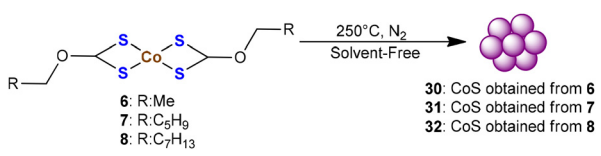

Scheme 6 Synthesis of nanoparticles **30–32** by thermolyzing the complexes **6–8** in solvent-free conditions.[42]

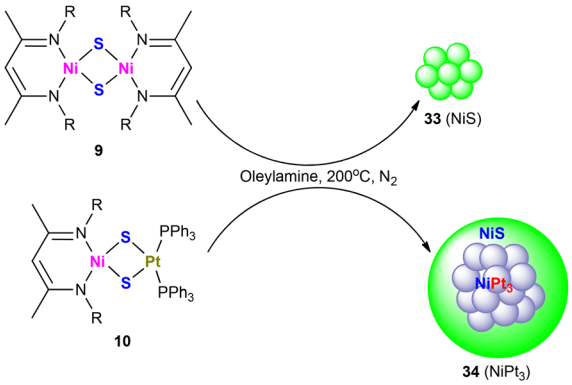

Scheme 7 Synthesis of nanoparticles **33** and **34**.[43]

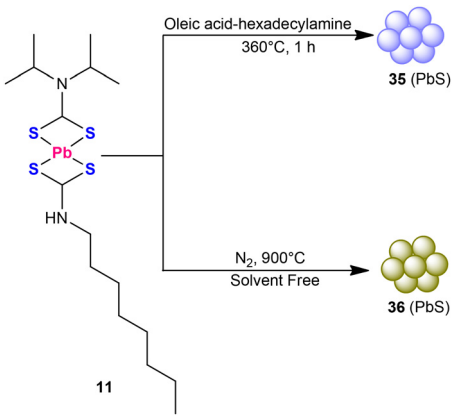

Scheme 8 Synthesis of nanoparticles **35** and **36** using complex **11**.[44]

comparison to the nanoparticles synthesized without any solvent, *i.e.*, **36**, with a size in the range of 3.16–5.95 nm.[44]

Nanocatalytic system **37** contains extremely thin Ag_2S nanowires. The wires crystallize in a monoclinic system. They are synthesized by the thermal degradation of molecular complex **12** at a moderate temperature (Scheme 9), *i.e.*, 140 °C in a mixture of octadecylamine, oleylamine, and *n*-decylboronic acid. These nanowires have an average diameter of 2.5 nm. However, their length is approximately 500–700 nm.[45]

3.2. Nanocatalysts as by-products: use of molecular complexes of organosulphur compounds as dispensers

There are some remarkable reports on the generation of nanocatalysts during the course of homogeneous catalysis by palladium complexes (Chart 4) of organosulphur compounds. These nanocatalysts are either nanosized binary phases of palladium sulphide or palladium(0) species. The properties of such nanocatalysts are greatly dependent on the molecular structure of the organosulphur ligands. These nanocatalysts, which are probably the true catalytic species in the reactions, can be isolated and separated from the reaction mixtures. They have a good shelf-life and can be stored.

Nanocatalysts **38** and **39** have palladium in a zero oxidation state.[46] The size (5–6 nm) of the particles in **39** is larger than that (3–5 nm) in **38**. Both of them are generated (Scheme 10) by complex **13** in which the Pd(II) is bound to the nitrogen of the 1,2,3-triazole unit of the ligand. When complex **13** is used to catalyze Suzuki–Miyaura coupling (Scheme 10), **38** is formed. When the same complex is used for the catalysis of Heck coupling reactions (Scheme 10), **39** is obtained.[46]

Nanocatalyst **40** has the quantum dots of palladium.[47] Their size is approximately 1–3 nm (Fig. 3). When complex **14** is used to catalyze the Suzuki coupling reaction, quantum dots are formed and released (Scheme 11) in the reaction mixture. They are stabilized by the fragments of the organosulphur ligand of complex **14**. They can be isolated and separated from the reaction mixture. They can be stored. They have the ability to show independent catalytic activity.[47]

Nanocatalytic system **41** has nanosized species of Pd(0).[48] Their size is approximately 7 nm. When Pd(II) complex **15** is used (Scheme 12) as a catalyst for the SMC reaction, the generation of **41** occurs (Scheme 12) in the reaction mixture. During the Suzuki coupling reaction, the nucleation of discrete palladium is likely to occur, leading to the formation of

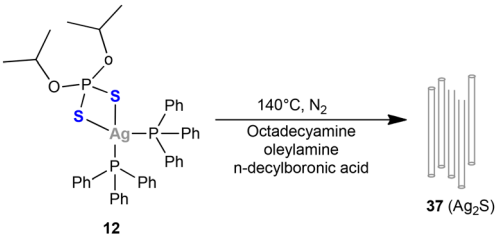

Scheme 9 Synthesis of the silver nanowire **37** using complex **12**.[45]

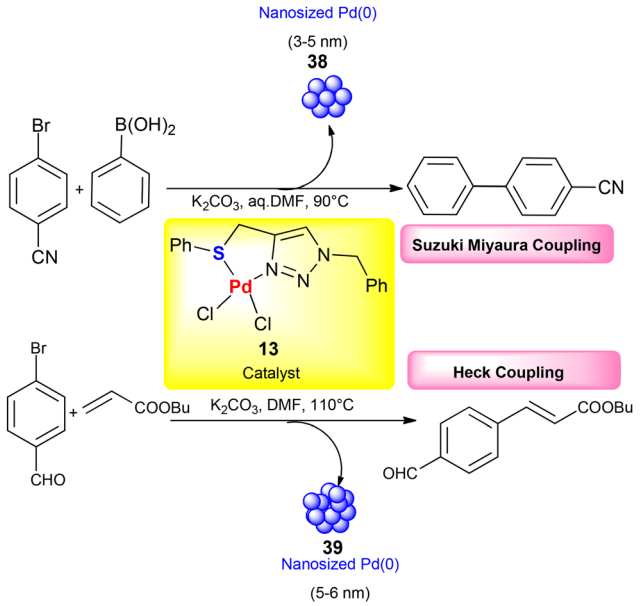

Scheme 10 Generation of nanoparticles **38** and **39** as by-products of the reactions (SMC and Heck coupling) catalyzed by the preformed molecular complex **13**.[46]

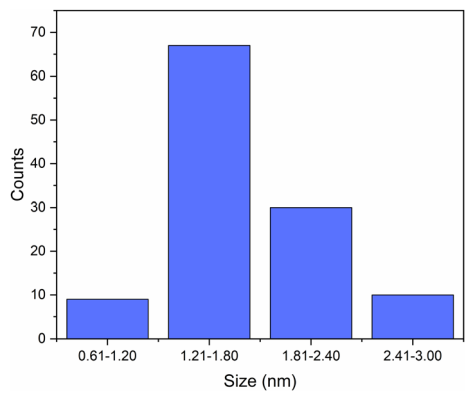

Fig. 3 Size distribution of the Pd(0) quantum dot nanocatalyst **40**. Reproduced from ref. 47 with permission from the Royal Society of Chemistry, Copyright {2013}.

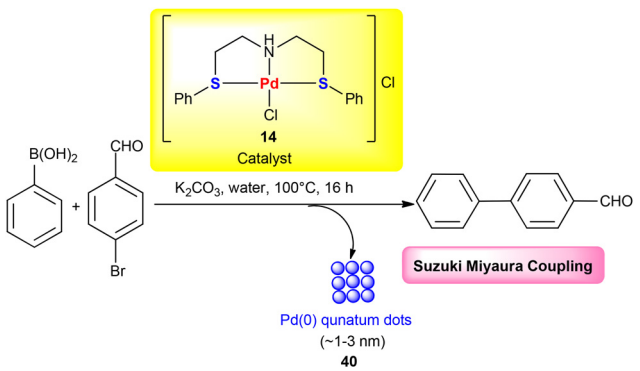

Scheme 11 Generation of nanoparticle **40** as a by-product of the SMC reaction catalyzed by the preformed molecular complex **14**.[47]

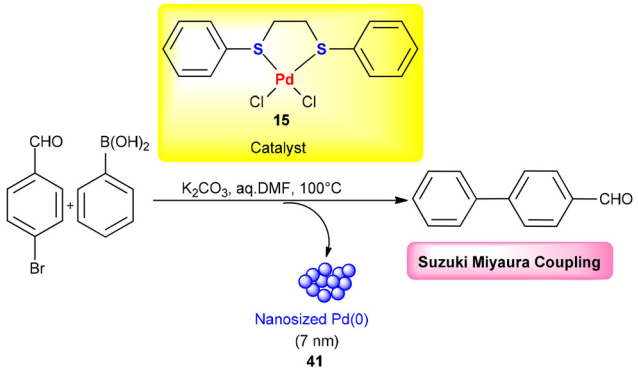

Scheme 12 Generation of nanoparticle **41** as a by-product of the Suzuki–Miyaura coupling reaction catalyzed by the preformed molecular complex **15**.[48]

peanut-shaped nanoparticles (Scheme 12). The size and shape of the nanoparticles depend on the nature of the coordinated atoms of the organosulphur ligand with palladium in complex **15**.[48]

Nanocatalysts **42** and **43** contain nanoparticles of palladium.[49] In the case of **42**, the size of the NPs is 5 nm. However, **43** contains NPs of a slightly larger size (6 nm). Moreover, **42** is generated (Scheme 13) by complex **16** during the catalysis of the Suzuki coupling reaction. In this complex, an organosulphur ligand is coordinated with palladium in bidentate mode. Palladium(II) complex **17** (in which an organosulphur ligand is coordinated to the metal in tridentate mode) leads to the formation of **43**. Both complexes have nitrogen as a hard donor and sulphur as a soft donor (Scheme 13) in their molecular structures.[49] Interestingly, in complex **17**, the ligand is a pincer-type (S, N, C donor) compound.[49]

When Pd(II) complexes **16** and **17** are used for catalyzing the Sonogashira coupling reaction, they lead to the formation of nanoparticles (Scheme 14) **44** and **45**, respectively. The difference in size between **44** and **45** is greater than that in the cases of **42** and **43**. The sizes of the nanoparticles are 3 nm and 6 nm for **44** and **45**, respectively.[49]

A variety of binary phases of Pd_xS_y (Pd_4S, Pd_3S, $Pd_{2.8}S$, $Pd_{16}S_7$, PdS, and PdS_2) are known. The majority of such phases are prepared by gas sulphuration with H_2S–H_2.[50–56] Moreover, **46** and **47** are the nanoparticles of the different binary phases of palladium sulphide. Additionally, **46** contains the nanoparticles of Pd_4S (Scheme 15).[57] In addition, **47** has a different composition. Its nanoparticles are made up of Pd_5S_2 (Scheme 15). They have significant differences in their sizes. The sizes of these nanoparticles are 19 nm and 5 nm for **46** and **47**, respectively.[57] The structure of Pd_4S was reported in 1962.[58] It is isostructural with Pd_4Se. The electrical conductivity of Pd_4S is similar to that of the metal,[59,60] but its tendency for the permeability of H_2 is different from that of the metallic Pd.[61,62] In the recent past, palladium sulphides have attracted the attention of chemists. Due to the interactions between Pd and S, their physicochemical properties are unique. Such properties include tunable catalytic behaviour, enhanced electron density modulation and improved thermal stability.[63] Their catalytic applications have not been given sufficient attention. Only a few reports on Pd_4S exist to understand its catalytic potential,[64,65] electrocatalytic potential,[66,67]

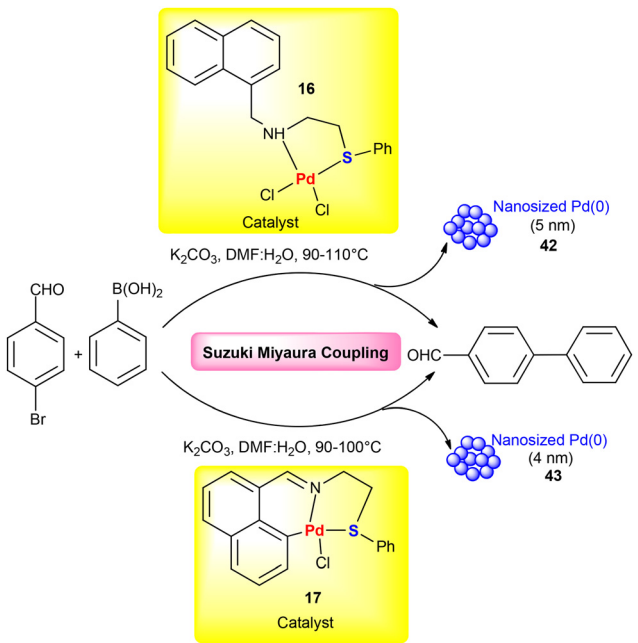

Scheme 13 Generation of nanoparticles **42** and **43** as by-products of the SMC reaction catalyzed by the preformed molecular complexes **16** and **17**.[49]

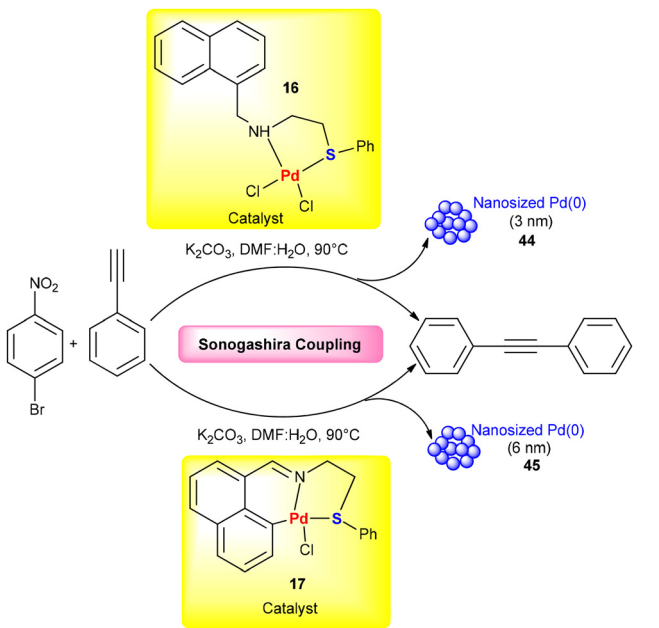

Scheme 14 Generation of nanoparticles **44** and **45** as by-products of the Sonogashira coupling reaction catalyzed by the preformed molecular complexes **16** and **17**.[49]

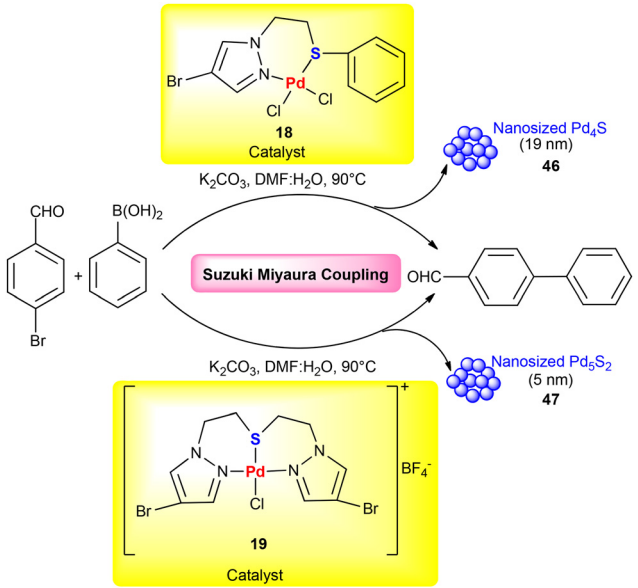

Scheme 15 Generation of nanoparticles **46** and **47** as by-products of the SMC reaction catalysed by the preformed molecular complexes **18** and **19**.[57]

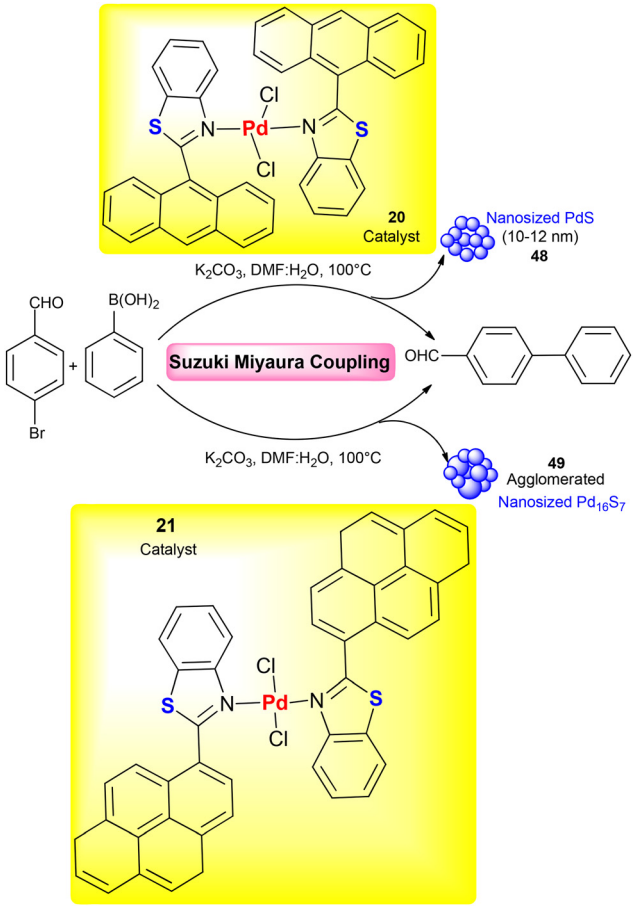

Scheme 16 *In situ* generation of nanoparticles **48** and **49** during the Suzuki–Miyaura coupling reaction using the preformed molecular complexes **20** and **21**.[73]

photocatalytic potential[59] and hydrogen permeability.[62] It has been found to show catalytic potential for selective gas phase alkyne hydrogenation,[64] liquid phase alkyne hydrogenation,[54,63] Suzuki coupling,[65] oxidation of methane[68] and oxygen reduction reaction.[66] As far as the methodologies of its synthesis are concerned, gas sulphuration with H_2S–H_2 [50–56] has also been reported as a method for its synthesis. It has also been synthesized using direct methods. However, such methods are challenging due to the harsh reaction conditions typically required.[52,53,62,68] The SSP route has rarely been reported for this.[66] To overcome these limitations, single-source precursor (SSP) methodologies have emerged as elegant and controllable strategies for the synthesis of metal chalcogenide nanomaterials.[69–72] Another interesting approach for its synthesis is *in situ* generation. Moreover, **46** and **47** are generated (Scheme 15) by complexes **18** and **19** during the catalysis of the Suzuki–Miyaura coupling reaction, respectively. Complex **19** has a tridentate ligand with two nitrogen and one sulphur donor atom (Scheme 15), and complex **18** has a bidentate (N, S donor) ligand.[57] Interestingly, the nanoparticles generated *via* these complexes are not Pd(0) nanoparticles; they are Pd_4S (**46**) and Pd_5S_2 (**47**).[57]

Nanocatalysts **48** and **49** also contain the binary phases of palladium sulphide.[73] Thus, **48** contains the nanoparticles of PdS, which are 10–12 nm in size. However, **49** has the nanoparticles of $Pd_{16}S_7$, which are agglomerated (revealed by HR-TEM analysis). When the Suzuki–Miyaura coupling reaction is carried out using Pd(II) complexes **20** and **21** (Scheme 16) as catalysts, **48** and **49** are generated. These nanoparticles are isolated and separated for their independent use as the catalysts.[73]

3.3. Use of organosulphur compounds as stabilizers for the development of nanocatalysts

The synthesis of nanoparticles can be achieved through various techniques, such as sol–gel,[74–79] hydrothermal,[80–82] microemulsion,[83,84] chemical co-precipitation,[85–87] and spray pyrolysis.[88,89] The science of nanoparticles hinges on two key factors: achieving the development of the nanoparticles with controlled size and shape, and rendering them the potential for specific applications. Such applications also include catalysis and electrocatalysis. Controlled size and shape are primarily achieved through the use of stabilizing agents, such as ligands (thiols, amines, and phosphines), surfactants (ammonium salts), and polymers (polyvinyl alcohols). The selectivity[6,7,15,16] and reactivity of nanoparticles play crucial roles in influencing the outcome of a reaction. The activity is dependent on many factors, including the surface area of nanoparticles. The involvement of inter-atomic interactions and the adjustment of under-coordinated/less coordinated surface atoms constitute the basis on which the properties of nanomaterials may be tuned. Such a possibility is rarely present in their bulk counterparts. Reduction in atomic

coordination significantly impacts the performance of surfaces, nano-solids, and amorphous solids in terms of bond relaxation and energy.[90,91]

The stability of nanoparticles against aggregation can be achieved using thermodynamic and kinetic approaches. The thermodynamic approach is adopted to suppress Ostwald ripening by minimizing the difference in chemical potential and surface energy between the nanoparticles (NPs).[92] On the basis of the results of the study on the thermodynamic behaviour of supported metal particles in various reaction environments, a general strategy has been suggested for the inhibition of the sintering of such NPs through theoretical calculations.[92] In this study, it has been observed that the stability of the particles and the rate of Ostwald ripening are determined by their size and distribution. When the sizes of the NPs are in a narrow range and their distribution is homogeneous, they have similar chemical potential and surface energy. In such cases, the Ostwald ripening rate is very low. Moreover, this objective can be achieved using a support with high surface activation energy. Therefore, in the preparation of NPs with uniform size and distribution, the selection of a suitable support is crucial for enhancing the stability of supported nano-catalysts.[92] The kinetic approach provides the basis for the use of an external medium (such as high temperature or high pressure) to limit the size of the nanoparticles. The rate of aggregation can be determined using various techniques, such as spectral turbidimetry, time-resolved dynamic light scattering (TR-DLS), and fluorescence correlation spectroscopy (FCS).[93]

Organosulphur compounds have sulphur as the donor site. They behave as very good stabilizers in the development of metal nanoparticles.[24] Nanoparticles of palladium with high catalytic potential have been developed using such compounds as stabilizers. In this method, a source of palladium (*e.g.* Na_2PdCl_4) is reduced in the presence of an organosulphur compound, and catalytically active and stable nanoparticles of metal (Chart 5), which are stabilized with such a compound, are produced. Such nanoparticles can be isolated and stored. The stabilizing ligands play an important role in dictating the size, shape, dispersion, and inter-particle spacing of nanoparticles. These compounds also affect the catalytic efficiency and recyclability of the synthesized NPs through ligation. The stabilizer compounds, which have functional groups such as amine, alcohol, carbonyl, thiol, hydroxy and phosphine, inhibit strong chemisorptions to the metal surface.[94] Therefore, the stabilizing ligand must be strong enough to stabilize the nanoparticle but should not have extremely strong interactions that hinder the catalytic activity of the NPs.

Nanoparticles **50** and **51** are palladium nanoparticles stabilized by an organosulphur compound. They have been synthesized using **L17** (a reduced Schiff base) as a stabilizer (Scheme 17). The size of nanoparticles has been found to be in a range of 2–3 nm in **50** and 4–5 nm in **51**. The only difference between them is the ratio of metal and stabilizing ligand (Scheme 17), with **50** having a ratio of 1 : 1 (metal precursor : ligand), while **51** has a ratio of 1 : 4 (metal precursor : ligand).

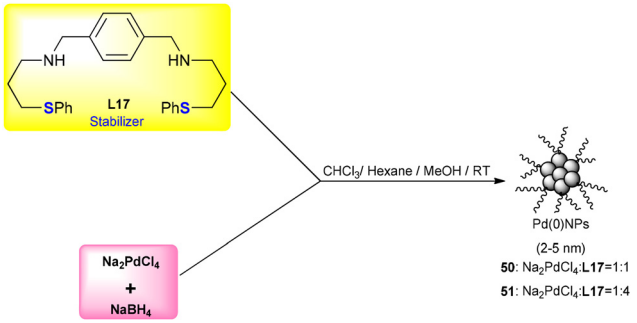

Scheme 17 Development of the Pd(0) nanoparticles **50** and **51** using the organosulphur ligand **L17** as the stabilizer.[95]

Ligand **L17** and palladium precursor Na_2PdCl_4 have been reduced using a reducing agent with different concentrations of metal and ligand to obtain NPs **50** and **51**.[95]

Ultrasmall nanoparticles **52**, **53** and **54** have been synthesized (Scheme 18) using ligand **L18** (containing the combination of sulphur and nitrogen donors) as a stabilizer.[96] Similar to the above-described NPs, the difference between these NPs is the ratio between the ligand and metal precursor. The reaction between ligand **L18** and Na_2PdCl_4 with different ratios (metal precursor : ligand) is utilized to obtain **52** (1 : 1), **53** (1 : 4) and **54** (4 : 1) NPs. The size of NPs has been found to be in the range of 1–2 nm for **52**, 2–3 nm for **53** and 4–6 nm for **54**.[96]

Nanoparticles **55–60** have been formed by *n*-didocosyl sulphide ligand **L16** (Scheme 19). The nanoparticles have been synthesized by the reaction between different palladium precursors [*i.e.*, Na_2PdCl_4, $Pd(OAc)_2$ and $Pd(MeCN)_2Cl_2$] and ligand **L16** with different ratios, such as 4 : 1, 1 : 2 and 1 : 4, for each precursor to give nanoparticles **55–60**. The NPs synthesized using Na_2PdCl_4 are found to be uniformly dispersed and hence have better catalytic activity among all.[97]

Pd–Ni-based nanocatalytic system **61** has been synthesized (Scheme 20) by reducing $Ni(NO_3)_2$ and $Pd(OAc)_2$ in the pres-

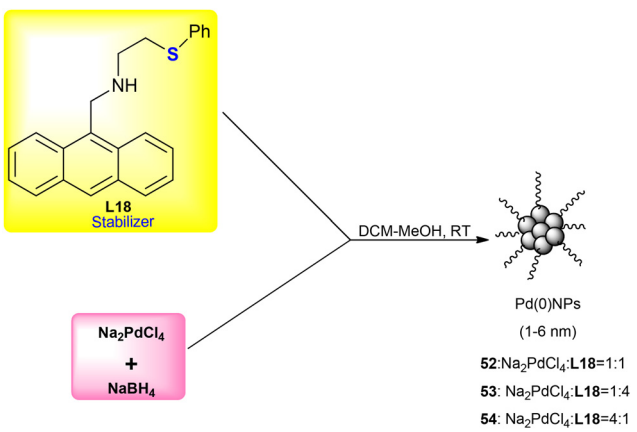

Scheme 18 Development of the Pd(0) nanoparticles **52–54** using the organosulphur ligand **L18** as the stabilizer.[96]

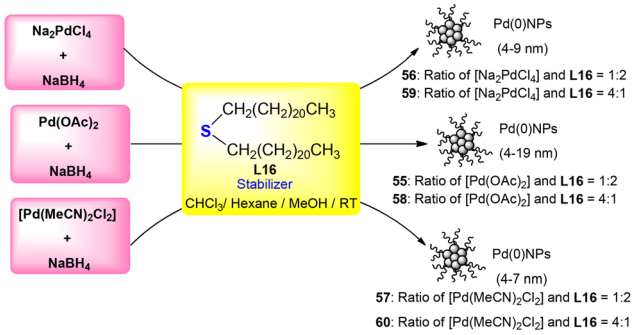

Scheme 19 Development of the Pd(0) nanoparticles **55–60** using the organosulphur ligand **L16** as the stabilizer.[97]

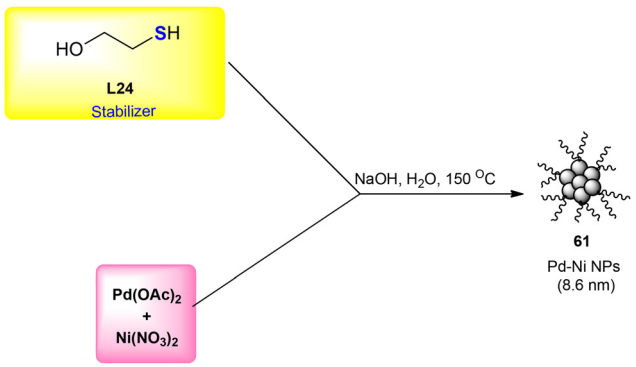

Scheme 20 Development of the Pd–Ni nanoparticle **61** using the organosulphur ligand **L24** as the stabilizer.[98]

ence of 2-mercaptoethanol (**L24**) as a stabilizer[98] in an aqueous basic (NaOH) solution. The pH of the mixture is maintained at around 11.5. The nanoparticles have been characterized using PXRD, SEM, IR and UV spectroscopic techniques. The majority of the nanoparticles have been obtained with less than 20 nm. The average particle size of nanoparticle **61** is 8.6 nm.[98]

4. Application in catalysis

4.1. Suzuki–Miyaura C–C cross coupling reaction

The Suzuki–Miyaura coupling reaction involves forming a C–C bond (Scheme 21) between an aryl halide and organoborane compounds.[99] This reaction is highly valued due to the simplicity of its process, such as mild conditions, the use of non-hazardous reagents, and its adaptability and utility across various industries, including the production of natural products and agrochemicals.[99,100] Extensive research has been conducted on the catalysts (developed using organosulphur compounds) for this reaction. Numerous nanocatalytic systems are also among them. Their applications provide quite interesting results.

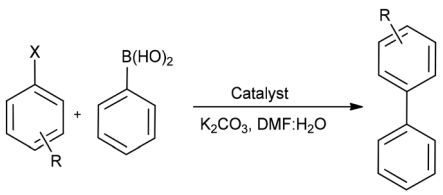

Scheme 21 Synthetic methodology for the Suzuki–Miyaura C–C coupling reaction.

4.1.1. Catalysis in short durations. Nanocatalysts such as **22**, **38**, **41–43** and **46–49** are very efficient for the Suzuki–Miyaura coupling reactions. All of them can catalyze this reaction within a few hours, *i.e.*, 2–3 hours.

$Pd_{16}S_7$ nanoflowers (**22**) are highly active nanocatalysts for the SMC reaction. Low catalyst loading (*i.e.*, 0.5 mol%) is sufficient for catalyzing this reaction within 3 hours. When 4-bromoacetophenone and phenyl boronic acid are reacted (Scheme 22) in the presence of its low (0.5 mol%) concentration, the coupled product is obtained with 91% yield.[37] It is recyclable up to four runs, and the yield obtained after the 4th cycle is 38%.[37]

Nanocatalyst **38** (developed from complex **13**) is very much useful.[46] It has the ability to catalyse the SMC reactions independently. The substrates including 4-bromobenzaldehyde, 4-bromoanisole and 4-bromoacetophenone react with phenylboronic acid in the presence of a very low quantity (nearly 5 mg) of this catalyst. The reaction between *p*-bromobenzaldehyde and phenyl boronic acid results in a 94% yield of the coupled product (Scheme 23) in a short duration of just 3 hours.[46]

However, nanocatalyst **47** (*i.e.*, NPs of Pd_5S_2) works at a relatively high (10 mg) catalyst loading for the same reaction (Scheme 23) and allows for the formation of the product in 02 hours.

Moreover, **41** (peanut-shaped nanoparticles) is used as a nanocatalyst for the SMC reaction (Scheme 24) of phenylboronic acid with 4-bromobenzaldehyde. Its low quantity (10 mg) gives the coupled products, *i.e.*, biphenyl-4-carboxaldehyde, in a very high (94%) yield in a very short duration of 02 hours at 100 °C. The reaction of 4-bromoanisole suffers from a low reaction rate due to the presence of the OMe group (an electron donating substituent) at the *para* position to the C–Br bond. It is converted to 4-methoxybiphenyl (the

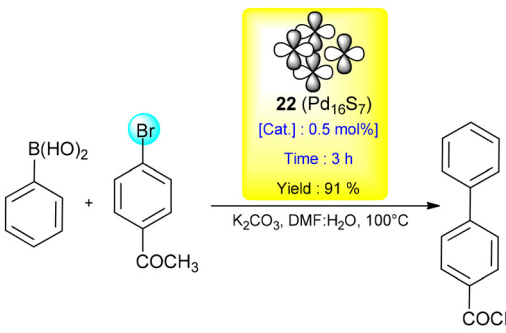

Scheme 22 Suzuki–Miyaura coupling using $Pd_{16}S_7$ (**22**) nanoflowers.[37]

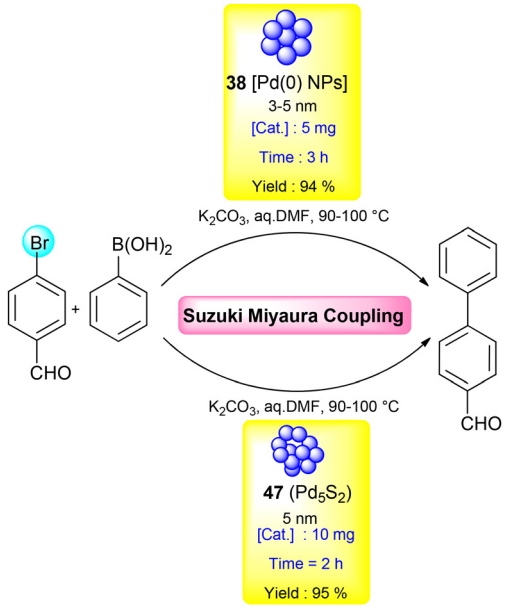

Scheme 23 Variation in the performance of *in situ* generated nanocatalysts **38** and **47** in the Suzuki–Miyaura coupling reaction.[46,57]

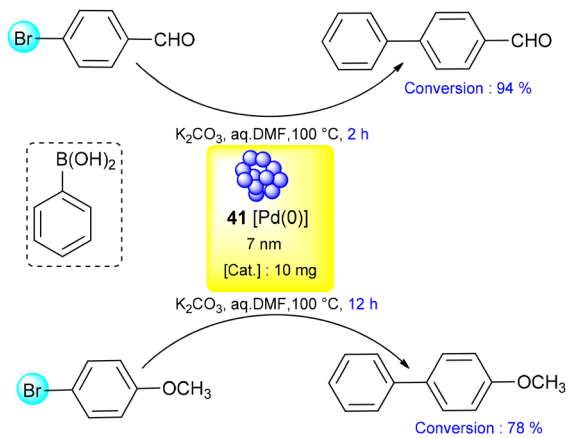

Scheme 24 Effects of electron-withdrawing and electron-donating substrates on the performance of nanocatalyst **41**.[48]

cross-coupled product) with a relatively low (78%) yield after a long duration of 12 hours under the same reaction conditions.[48]

Nanocatalysts **42** and **43** (generated by complex **16** and palladacycle **17**) also catalyze the Suzuki coupling reactions.[49] Their low quantity (2.0 mol%) allows the reactions to proceed and gives the coupled product with good yields, *i.e.*, 71–95%. Nanocatalyst **42** performs better than nanocatalyst **43** in all the coupling reactions. The size of **42** (5 nm) is slightly larger than that of **43** (4 nm). The particles of **42** are more dispersed than those of **43**. This could be the reason for the better activity of **42** in the coupling reactions. For example, when 4-bromobenzonitrile is reacted with phenyl boronic acid, the presence of **42** gives the product in a 91% yield. The same reaction gives the product (Scheme 25) in 81% yield in the presence of **43** under the same reaction conditions.[49]

Nanocatalysts **46** and **47** have also been independently utilized as catalysts for the SMC reactions. There is no significant variation between their catalytic performances. The coupling of 4-bromobenzaldehyde with phenyl boronic acid gave 92 and 95% yields within 2 hours (Scheme 23) in the presence of 10 mg of the nanocatalyst (*i.e.*, **46** and **47**, respectively).[57] The high surface to volume ratio and uniformity in distribution of NPs are likely to be among the reasons and the factors that are responsible for their enhanced catalytic activity.[57]

4.1.2. Green catalysis using ultrasonication. Nanocatalyst **61** has been utilized for the catalysis of the SMC reaction *via* a green method, *i.e.*, ultrasonication. This nanocatalyst catalyses the coupling reaction at 0.1 mmol catalyst loading. When 4-bromotoluene is reacted with phenylboronic acid (Scheme 26) under these conditions, the coupled product is obtained with a 94% yield within 5 minutes.[98]

4.1.3. Catalysis in green solvents. Nanocatalyst **40** (*i.e.*, the quantum dots of palladium) has shown potential for catalyzing

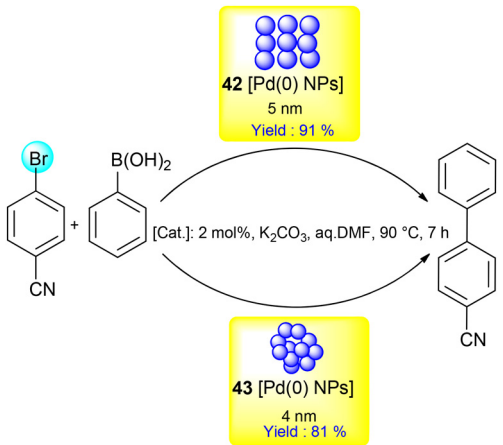

Scheme 25 Effect of the dispersion of NPs on the efficiency of the SMC reaction.[49]

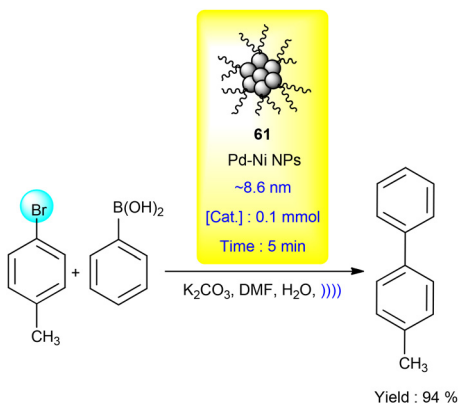

Scheme 26 Suzuki–Miyaura coupling reaction catalyzed by NP **61** *via* ultrasonication.[98]

the SMC reaction in green solvent, *i.e.*, water. This nanocatalyst (obtained from metal complex **14**) catalyzes the coupling reaction at 2.0 mol% catalyst loading at 100 °C. When 4-bromobenzoic acid is reacted with phenylboronic acid (Scheme 27) under these conditions, the coupled product is obtained with >99% yield in 05 hours. This nanocatalyst does not become inactive after the reaction. It can be reused for up to 2 cycles.[47]

4.1.4. Effect of agglomeration of nanoparticles on catalytic efficiency. Nanocatalysts **48** and **49** have been explored for their independent efficiency (Scheme 28) for the catalysis of the Suzuki–Miyaura coupling reaction.[73] When 4-bromobenzoic acid is reacted with phenyl boronic acid in the presence of 5 mg of the nanocatalyst, the coupled product is obtained with 92% and 68% conversion for **48** and **49**, respectively. This difference could be due to the agglomeration of nanoparticles in the case of **49**.[73]

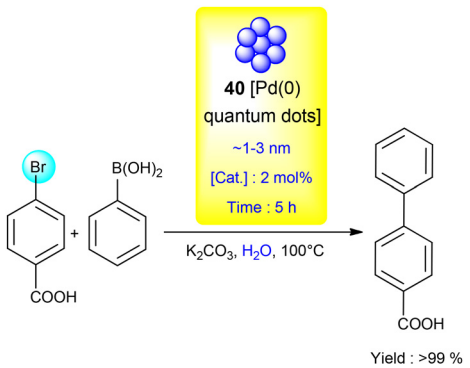

Scheme 27 Suzuki–Miyaura coupling reaction catalyzed by NP **40** in water.[47]

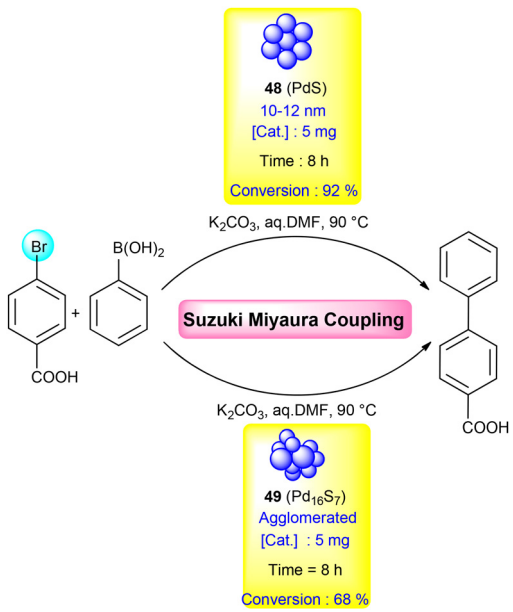

Scheme 28 Effect of agglomeration on the performance of *in situ* generated nanocatalysts **48** and **49** in Suzuki–Miyaura coupling.[73]

4.1.5. Chloroarenes as substrates. It is the most difficult task for a catalyst to convert chloroarenes into coupled products in the Suzuki–Miyaura coupling (SMC) process. Nanocatalysts **50** and **51** have this ability (Scheme 29) to perform such a task.[95] The reactions are performed (Scheme 29) at 0.1 mol% catalyst loading to achieve the product in an outstanding yield, *i.e.*, >99%, in a short reaction time. Moreover, **51** takes 2 hours, and **50** gives similar results in 03 hours (Scheme 29). Hence, it can be concluded that nanocatalytic system **51** is more efficient than **50**. A recyclability test of nanocatalytic system **51** is also performed using 4-bromobenzaldehyde as one of the reactants in the reaction. The results of such a test reveal that it has good recyclability up to three cycles, and an average yield of 41% is obtained in the third cycle.[95]

4.1.6. Bromoarenes as substrates. It is relatively easy to convert bromoarenes into cross-coupled products in the Suzuki reaction. Nanocatalysts (*i.e.*, palladium nanoparticle **52–54**), which have good dispersion and stabilization, are efficient catalysts for the SMC reactions involving bromoarenes. The stabilizer used during its development is **L18**,[96] which contains a thioether donor site. It exhibits the efficiency for the catalysis of the reactions of such substrates.[96] They are used in low quantities (5 mg) and give the coupled products in good yields (*i.e.*, 68–99%). Among them, **53** has shown the least potential. This could be because in nanoparticle **53**, the ligand-to-metal precursor ratio is 4 : 1. Palladium is present in low concentrations, and the stabilizing ligand is present in high concentrations. Ligands could encapsulate the palladium (or the active sites) in such a way that the reactants could not reach the active sites efficiently. Nanocatalyst **52** has shown the highest efficiency (Scheme 30) and reactivity among the three NPs, *i.e.*, **52–54**, possibly due to their relatively small size and high uniformity in the dispersion.[96]

Nanocatalytic system **55–60**, developed by the reduction method using **L16** as the stabilizer, has the potential for catalysing the SMC reactions of bromoarenes.[97] Among them, the highest activity is exhibited by nanoparticle **56**, the development of which is carried out using sodium tetrachloropalladate (Na_2PdCl_4). They have very high uniformity in size and

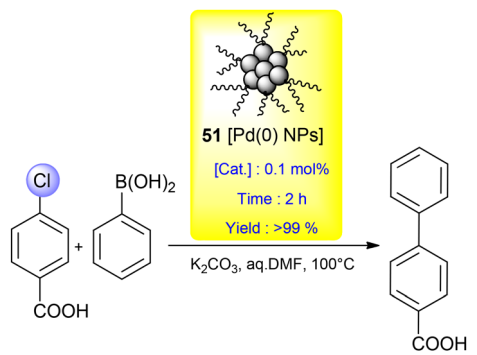

Scheme 29 Suzuki–Miyaura coupling reaction catalyzed by nanocatalyst **51**.[95]

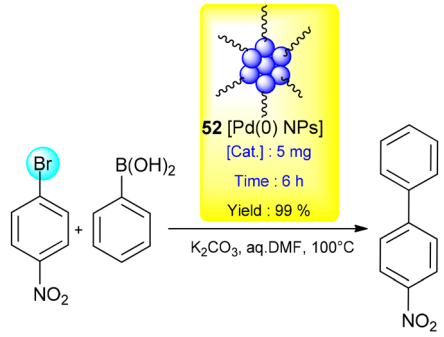

Scheme 30 Suzuki–Miyaura coupling reaction catalyzed by nanocatalyst **52**.[96]

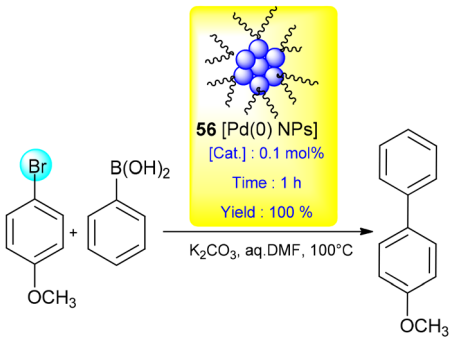

Scheme 31 Suzuki coupling reaction catalyzed by nanocatalyst **56**.[97]

dispersion. When 4-bromoanisole and phenylboronic acid are reacted (Scheme 31) at 0.1 mol% catalyst loading, nanocatalyst **56** gives an excellent yield (*i.e.*, ≥99%) in a short reaction time of 1 hour. However, **55**, **57**, **58**, and **59** give moderate yields. Moreover, **60** has shown negligible efficiency for the reaction, and the product is obtained in trace amounts. The order of efficiency of these catalysts has been found to be **56** > **58** > **57** > **59** > **55** > **60**.[97]

4.2. Heck coupling reaction

The Heck coupling reaction forms substituted olefins (Scheme 32) by the treatment of an aryl halide with terminal alkenes.[101,102] This reaction is feasible under mild conditions and can accommodate a variety of functional groups, such as aldehyde, amines, esters and nitro groups, without compromising the results (*i.e.*, high yields of the products).[103] It is widely used in the production of fine chemicals.[101,102] Organosulphur compounds are often used to develop various types of catalytic systems for this reaction.[104] Like the Suzuki coupling reaction, it has also been observed in this reaction

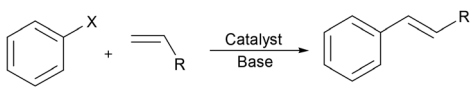

Scheme 32 Synthetic methodology for the Heck coupling reactions.

that some nanoparticles or nano species are generated *in situ* during the catalysis of this reaction with preformed metal complexes. Such nanoparticles (*e.g.*, **39**) can be isolated from the reaction mixtures and stored for their applications as independent nanocatalysts.[46]

Moreover, **39** is utilized for the Heck coupling reaction of aryl bromides (such as 4-bromobenzaldehyde and 4-bromoacetophenone), which have highly active electron withdrawing groups with *n*-butyl acrylate. When 4-bromobenzaldehyde and *n*-butyl acrylate are reacted (Scheme 33) in the presence of 30 mg of the catalyst, *i.e.*, **39**, the yield of the product obtained is 75%. This nanocatalyst is unable to convert 4-bromoanisole into the product.[46]

4.3. Sonogashira coupling

Sonogashira coupling is a reaction in which a terminal alkyne and an aryl halide combine (Scheme 34) with each other through the formation of a new C–C bond. This method is commonly used to produce pharmaceuticals, natural products, organic compounds and nanomaterials.[105]

Like the Suzuki and Heck coupling reactions, during the catalysis of Sonogashira coupling reactions by Pd(II) complexes **16** and **17**, Pd(0) nanoparticles, *i.e.*, **44** and **45**, are generated *in situ* in the reaction mixture.[49] These nanoparticles (*i.e.*, **44** and **45**) are isolated and stored. They can be used independently for catalysis. They produce moderate to high yields (ranging from 42 to 91%) in Sonogashira coupling reactions. When 1-bromo-4-nitrobenzene is reacted with phenyl acetylene utilizing a 2.0 mol% concentration of the nanocatalyst without

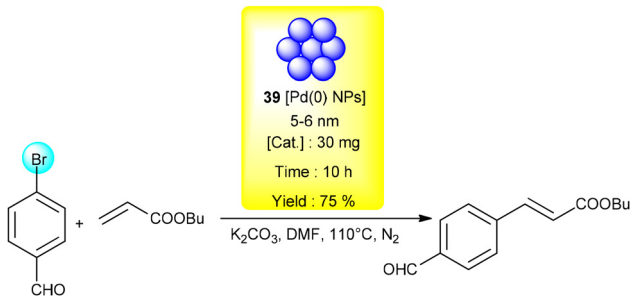

Scheme 33 Heck coupling reaction using the nanocatalytic system **39**.[46]

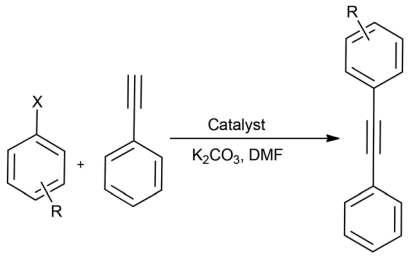

Scheme 34 Synthetic methodology for the Sonogashira coupling reactions.

the addition of any co-catalyst, **44** and **45** (Scheme 35) give the desired product in 76% and 91% yields, respectively.[49] This high performance of **45** could be attributed to the smaller size of Pd(0) NPs in this case.

4.4. *O*-Arylation of phenol

In *O*-arylation, phenol combines with aryl halides (Scheme 36) to form diaryl ethers. This type of C–O coupling is widely used in the production of polymers[106] and agrochemicals.[106] Many palladium-based nanocatalytic systems have been developed for this reaction.[106]

Nanocatalyst **22** (*i.e.*, flower-shaped nanoparticles of $Pd_{16}S_7$), obtained from palladium complex **1** using the single source precursor method, has the ability to carry out the catalysis of this reaction.[37] This nanocatalyst is used for the coupling of phenol with a variety of aryl bromides at a low catalyst loading of 0.5 mol% under mild reaction conditions. When 1-bromo-4-nitrobenzene and phenol are reacted at 100 °C (Scheme 37) in the presence of a 0.5 mol% concentration of the catalyst, the coupled product is obtained with a 92% yield. The bromides with electron donating groups, such as $-CH_3$, –H or $-OCH_3$, show less reactivity compared to the ArBr, which has electron withdrawing groups, such as –CHO, $-NO_2$, –CN or $-COCH_3$.[37]

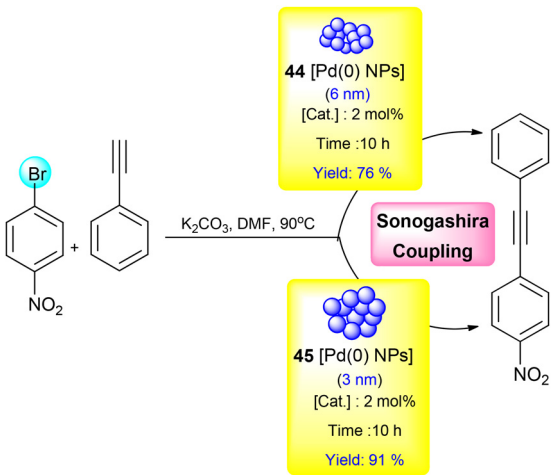

Scheme 35 Variation in the performance (due to the size of nanoparticles) of *in situ*-generated nanocatalysts **44** and **45** in Sonogashira coupling.[49]

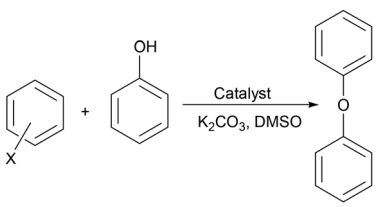

Scheme 36 Synthetic methodology for the *O*-arylation of phenol.

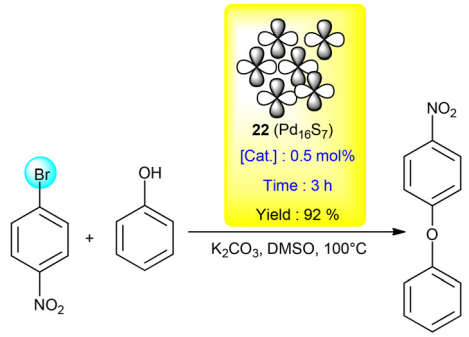

Scheme 37 *O*-Arylation of phenol using nanocatalyst **22**.[37]

4.5. Cross-dehydrogenative coupling (CDC)

Cross-dehydrogenative coupling is a chemical reaction (Scheme 38) that forms a C–C bond or C–heteroatom bond by removing two hydrogen atoms from two compounds.[107,108] The formation of such bonds is significant in the synthesis and functionalization of complex organic molecules, including natural products and pharmaceuticals. CDC reactions are often catalyzed by metals and can proceed under mild conditions, offering a versatile and efficient approach to C–C or C–heteroatom bond formation in organic synthesis.[107]

Nanocatalytic system **23** has been explored for cross dehydrogenative coupling (Scheme 39) of *N*,*N*-dimethylbenzylamines with azoles under solvent free conditions.[38] When *N*,*N*-dimethyl-1-phenylmethanamine and 1*H*-1,2,3-triazole are reacted together in the presence of 1.0 mol% concentration of this catalyst (Scheme 39), the desired product is obtained with a 74% yield. This catalyst is also reusable for up to 5 reaction cycles with only a slight loss in activity. Depending on the substrate used, the yield of the product can reach up to 89% in the case of catalysis with the **23**.[38]

The proposed mechanism of the reaction using nanocatalyst **23** is depicted in Scheme 40.[38] In the first step, copper-

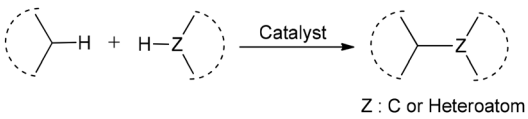

Scheme 38 Synthetic methodology for cross-dehydrogenative coupling (CDC).

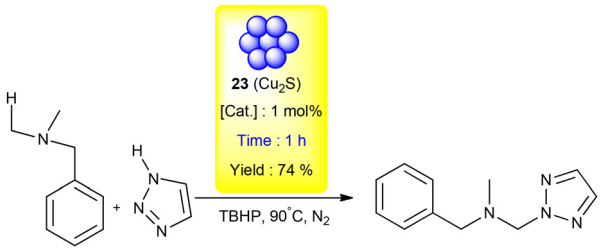

Scheme 39 Cross-dehydrogenative coupling reaction catalyzed by nanocatalyst **23**.[38]

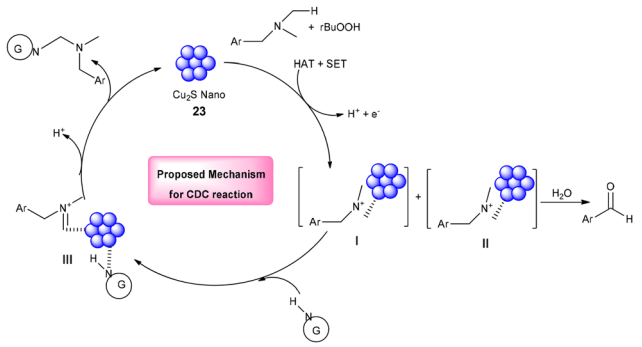

Scheme 40 Proposed mechanism of cross-dehydrogenative coupling reaction catalyzed by nanocatalyst **23**.[38]

catalyzed decomposition of *tert*-butyl hydroperoxide (TBHP) takes place (Scheme 40) to generate a *tert*-butoxyl radical. A radical cation is generated *via* a single electron transfer (SET) from an amine. After this step, the abstraction of the sp^3 hydrogen of the radical cation takes place to generate iminium-type intermediate **I** or **II** (Scheme 40). In the next step, triazole/carbazole reacts with compound **I**, which results in the formation of compound **III** (Scheme 40). In the last step, the C–N coupled product is formed (Scheme 40) *via* a nucleophilic substitution reaction between the azole and iminium ion, regenerating nanocatalyst **23** for the next catalytic cycle. The organosulphur compound (*i.e.*, **2**) utilized for the synthesis of nanocatalyst **23** does not directly influence the reaction mechanism; however, it has a role in the development of the particular binary phase Cu_2S nanoparticles (**23**), which are used as catalysts for this reaction.[38]

5. Applications in electrocatalysis

Metal sulphides have emerged as highly promising catalysts in electrochemical processes over the last decade owing to their diverse range of properties. Such properties encompass high surface area, excellent electrical conductivity, metallic structure and unique morphology. It is worth noting that these materials have demonstrated high potential in electrocatalytic reactions, like the hydrogen evolution reaction (HER), oxygen evolution reaction (OER) and overall water splitting. These properties make them useful and crucial for advancement in electrocatalysis.

5.1. Hydrogen evolution reaction (HER)

Nanocatalysts **25**, **26**, **33**, **34** and **37** are interesting species for the hydrogen evolution reaction (HER) (Table 1). This reaction involves the electrochemical process in which molecular hydrogen is generated (Scheme 41).

Overpotentials of 132 mV and 153 mV have been observed when **25** and **26** are employed as catalysts (Scheme 39) for the hydrogen evolution process.[40] These are cobalt sulphide (CoS) nanoparticles. The value of the Tafel slope is 159 mV dec^{-1} for **25**. However, this value is slightly low (154 mV dec^{-1}) for **26**. When they are applied for hydrogen evolution studies, a standard three-electrode system [with samples on nickel foam as the working electrode, platinum wire as the counter electrode, and saturated calomel electrode (SCE) as a reference in 1.0 M KOH electrolyte] is used for the experiments. Nyquist plots at various overpotentials were also obtained and understood. It can be noticed that with the increase in potential, the curves from the Nyquist plots begin to transform from a straight line into a slightly semicircle for both **25** and **26**. This is because a high level of potential results in a faster reaction, showing enhanced activity of CoS electrodes (*i.e.*, electrocatalysts **25** and **26**).[40]

The potentials of **33** and **34** have also been studied in electrocatalysis for the HER.[43] When a reductive potential is applied at a rate of 1 mV per second, nanocatalyst **34** shows

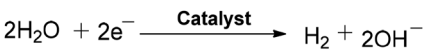

Scheme 41 Synthetic methodology for molecular hydrogen generation.

Table 1 Current density, overpotential values and Tafel slopes exhibited by various metal sulphides towards the hydrogen evolution reaction (HER) and oxygen evolution reaction (OER)

S. no.	Catalyst	Current density (mA cm^{-2})	Overpotential towards the HER (mV)	Tafel slope for the HER (mV dec^{-1})	Overpotential towards the OER (mV)	Tafel slope for the OER (mV dec^{-1})	Ref.
1.	**24** (Cu_9S_5)	10	—	—	293	67 ± 3	39
2.	**25** (CoS S rich)	10	132	159	307	96	40
3.	**26** (CoS Co rich)	10	153	154	276	82	40
4.	**27** (NiS hexagonal nanocrystals)	50	273	—	389	—	41
5.	**28** (NiS hexagonal nanocrystals)	50	259	—	389	—	41
6.	**29** (NiS rhombohedral nanocrystals)	50	231	—	371	—	41
7.	**30** (CoS obtained from **6**)	10	200	126	325	77	42
8.	**31** (CoS obtained from 7)	10	232	138	361	67	42
9.	**32** (CoS obtained from **8**)	10	235	101	339	77	42
10.	**33** (NiS)	−10	107	71	—	—	43
11.	**34** ($NiPt_3$ coated with NiS)	−10	12	31	—	—	43
12.	**37** (Ag_2S)	10	−88	52	—	—	45

overpotential values of just 12 mV and 73 mV at the HER current densities of −10 and −100 mA cm^{-2}, respectively. However, **33** shows the efficiency towards the HER with overpotential values of 107 and 229 mV at current densities of −10 and −100 mA cm^{-2}, respectively. The values of Tafel slopes provide important information to enhance understanding and compare kinetics. This value is 71 mV dec^{-1} for **33** and 31 mV dec^{-1} for **34**. Chronoamperometry has also been performed on **33** and **34** coated nickel foam electrodes. Moreover, **34** exhibits consistent stability over 24 hours at the HER overpotentials of 12 and 75 mV. However, **33** requires a greater overpotential (107 mV) to maintain a steady current density of −10 mA cm^{-2} for two days.[43]

In addition, **37** (*i.e.*, Ag_2S nanowires) exhibits strong HER activity in comparison to the bulk form of Ag_2S.[45] It is ultrathin in size. It has high electrocatalytic activity (Scheme 42), a highly reduced level of resistance, and significantly high durability for the HER process.[45] At 10 mA cm^{-2}, it has a substantially reduced overpotential of −88 mV, while bulk Ag_2S has an overpotential of 242 mV (Scheme 42) at the same current density. Furthermore, **37** has a Tafel slope value of 52 mV dec^{-1}, indicating a more effective HER mechanism than the bulk material (bulk counterpart) for which 141 mV dec^{-1} is the value of the Tafel slope. An electrochemical impedance spectroscopic (EIS) study has also been carried out. The results of this study reveal that **37** has a lower charge transfer resistance (51.4 Ω) than the bulk material (138.2 Ω), indicating greater electrocatalytic activity. When **37** is subjected to chronoamperometric studies, it is found to demonstrate outstanding stability, with a reduction of only 11% in starting current density after 12 hours. The electrochemically active surface area (ECSA) of **37** is relatively larger than the bulk Ag_2S. This is likely to be the main reason for its enhanced electrocatalytic activity.[45]

5.2. Oxygen evolution reaction (OER)

24, **25** and **26** are interesting nanosized species for the oxygen evolution reaction (OER) (Table 1). This reaction involves the electrochemical process in which molecular oxygen is generated (Scheme 43) and evolved.

The potential of nanocatalytic system **24** has been studied for the OER.[39] It is deposited on a highly conducting nickel foam electrode. The value of the overpotential achieved using this material is only 293 mV (Scheme 44) to obtain a current density of 10 mA cm^{-1}. In the past, CuO and Cu nanoparticles were synthesised and deposited on NF[39] in the same manner as adopted in the case of **24**. The values of Tafel slopes are used to evaluate the OER kinetics for **24**/NF, CuO/NF, and Cu/NF, which are 67 ± 3 mV dec^{-1}, 92 ± 4 mV dec^{-1}, and 146 ± 3 mV dec^{-1}, respectively. Tafel slope value for **24**/NF is lower than that for CuO/NF and Cu/NF. This indicates that **24**/NF has high ease for electron transport, favourable electrocatalytic reaction kinetics, and considerable catalytic activity towards the OER. In addition, **24**/NF has a high ECSA (0.89 cm^2), indicating the presence of more active OER sites, as well as a low charge transfer resistance. This is also an indication of the increased charge transport across the electrode/electrolyte and *vice versa*. Its long-term durability has been assessed using chronoamperometry at 1.55 V (*vs.* RHE) and maintained at a current density value ≥10 mA cm^{-2} for 12 hours, demonstrating the catalyst's intrinsic stability over a longer run.[39]

Moreover, **25** and **26** exhibit the ability to carry out the oxygen evolution reaction (OER), with overpotentials of 307 mV and 276 mV, respectively.[40] The values of Tafel slopes for **25** and **26** are 96 and 82 mV dec^{-1}, respectively. It can be observed that the value of the Tafel slope for **26** is lesser than that of **25**. This indicates greater electrocatalytic performance (Scheme 44) of **26** due to faster electron transfer and OER kine-

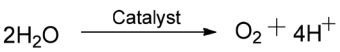

Scheme 43 Synthetic methodology for oxygen generation.

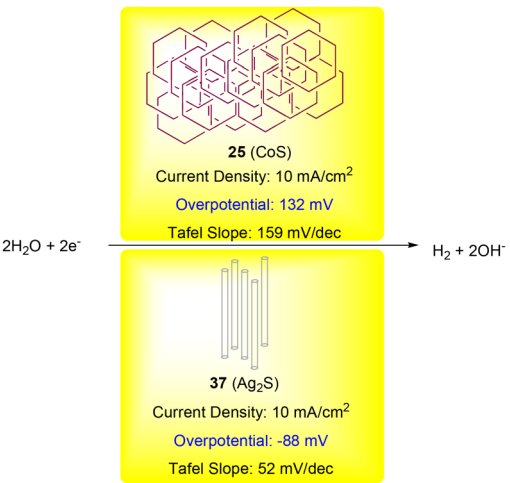

Scheme 42 Electrocatalytic HER using nanocatalysts **25** and **37**.[40,45]

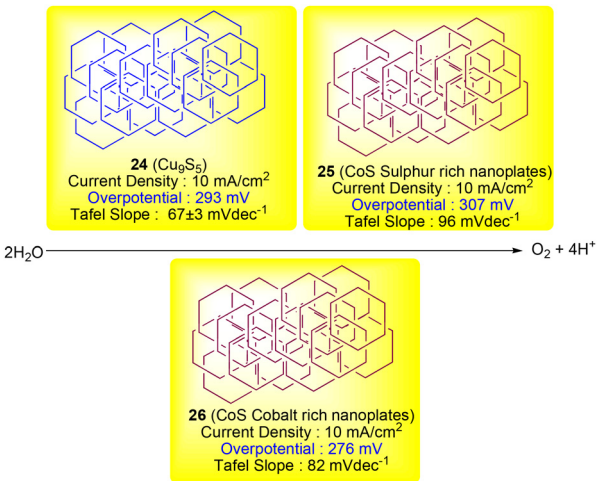

Scheme 44 Electrocatalytic OER using nanocatalysts **24**, **25** and **26**.[39,40]

tics in this case. Electrochemical impedance spectroscopic (EIS) measurements at various potentials were also performed and studied using Nyquist plots. Additionally, **26** has a smaller semicircle diameter at 0.45 V. This also indicates a reduced level of charge transport resistance and a quick rate of electron transfer. As a result, enhanced electrocatalytic performance and quick electron transfer are observed in the case of **26**, and it shows an improved electrocatalytic performance.[40]

5.3. Overall water splitting

27, **28**, and **29** have nickel sulphide (NiS) nanoparticles, and they show electrocatalytic performance (for overall water splitting) for the oxygen evolution reaction (OER).[41] When the polarisation curves are compared using linear sweep voltammetry (LSV) at a current density of 50 mA cm^{-2}, it is noticed that **29** has the lowest overpotential of 371 mV, while the value of overpotentials for **27** and **28** is 389 mV. Thus, **29** also has superior electrochemical stability. Low potential variations of roughly 5 mV are present between the 1st and 1000th cycles of LSV at 50 mA cm^{-2}. The combination of low overpotential and high electrochemical stability demonstrates that **29** is an excellent electrocatalyst for the oxygen evolution process. Similarly, the electrocatalytic activities of nickel sulphide samples for the hydrogen evolution processes (HERs) have been investigated and understood. To obtain a current density of 50 mA cm^{-2}, **29** requires the lowest overpotential of 231 mV, while **27** and **28** have overpotentials of 273 mV and 259 mV, respectively. Interestingly, **29** outperforms the other samples in terms of efficiency for both processes, *i.e.*, the OER and HER. It is worth noting that **27** (with the millerite phase) is the most efficient in terms of charge storage efficiency. As a result, it can be concluded that different phases may perform differently in energy generation and storage applications.[41]

Nanocatalyst **30–32** has cobalt sulphide (CoS) nanoparticles. They have also been utilized for the study of overall water splitting processes.[42] Their electrocatalytic activity for the OER is investigated, studied and understood using LSV. The polarisation curves demonstrate that **30** has the lowest overpotential value (325 mV) at a current density of 10 mA cm^{-2}. They have quick and efficient reaction kinetics in electrocatalytic processes. The values of the Tafel slope for **30**, **31**, and **32** are 77 mV dec^{-1}, 67 mV dec^{-1}, and 77 mV dec^{-1}, respectively. When the nanosized electrocatalyst has small particles, it has a large active surface area, leading to an improvement in electrochemical behaviour and characteristics. All the three species display stable current density during the 18-hour long-term stability test. Nanocatalyst **30–32** has also been investigated for the hydrogen evolution process (HER). Moreover, **30** is the most effective electrocatalyst for the HER reaction, with a Tafel slope of 126 mV dec^{-1} and the lowest overpotential of 200 mV at 10 mA cm^{-2}. The size and surface area of its nanoparticles also have a direct and visible effect on HER efficiency. For both the OER and HER reactions, **30** exhibits better efficiency in comparison to **31** and **32**. The studies reveal that **30** has a reduced level of over potential of 325 mV for the OER and 200 mV for the HER at a current density of 10 mA cm^{-2}.[42]

6. Challenges and alternative approaches

Nanocatalytic systems developed utilizing organosulphur compounds offer the advantage of being recyclable and reusable for multiple cycles without any significant loss in catalytic activity. Advancements in this field can lead to the development of a comparatively stable, highly active, and efficient catalytic system, as the bonding of sulphur with metal is likely to create favourable electronic properties on the metal centre with a stable environment for catalytic reactions. Moreover, the scope of catalytic systems (developed using organosulphur compounds) encompasses a wide range of chemical transformations, such as Heck coupling, cross-dehydrogenative coupling (CDC), Suzuki coupling and *O*-arylation of phenols. There are several other chemical transformations to which the use of such nanocatalysts can be extended. In the field of electrocatalysis, although various noble and non-noble metal sulfides have been utilized, there is still a need for the development of novel electrocatalytic systems with improved activity for electrochemical reactions using organosulphur compounds. Therefore, diverse approaches can be followed for synthesising novel organosulphur compounds and for applying them in the development of nanocatalytic systems. The potential of such systems in various fields, such as catalysis and electrocatalysis, can be harnessed at a wider level.

7. Future scope and conclusion

This article focuses on advancements related to the synthesis and employment of organosulphur compounds in the field of the development of nanocatalysts and electrocatalysts. Nowadays, nanocatalysis is a crucial aspect of both academic and industrial research and development. Nanocatalysts are obtained using organosulphur compounds using three distinct methods, specifically the single source precursor route, *in situ* generation during homogeneous catalysis of coupling reactions by preformed sulphur ligated palladium complexes, and the reduction method involving the utilization of organosulphur compounds as stabilizers. This article delves into the applications of nanocatalytic systems in catalyzing various chemical transformations, including Suzuki–Miyaura coupling, Heck coupling, Sonogashira coupling, *O*-arylation of phenol, and cross-dehydrogenative coupling (CDC). It also highlights their utilization in electrochemical applications, such as the hydrogen evolution reaction (HER), oxygen evolution reaction (OER), and overall water splitting. This article provides a critical analysis of these catalytic systems in terms of the advantages of their use. It also emphasizes the potential and scope for further extensive and in-depth studies on the design and application of such catalysts, highlighting the immense possibilities in the field of catalysis for various other transformations and electrocatalysis. It has been demonstrated that small-sized and highly dispersed nanoparticles are more efficient in catalysis. In the reduction method, when Na_2PdCl_4

is used as a precursor, it gives more uniformly dispersed nanoparticles than those obtained using $Pd(OAc)_2$ and $Pd(MeCN)_2Cl_2$ as the source of palladium. Therefore, Na_2PdCl_4 is the better choice in terms of precursor for the development of palladium containing nanocatalysts using organosulphur compounds as the stabilizers and reduction process as the method. In the field of catalysis, the use of mainly palladium-based nanocatalysts has been discussed. There is a scope of development and use of other metal nanoparticles, such as Ni and Cu, using similar strategies. The development of such nanoparticles using the reduction method or the single source precursor (SSP) route would be interesting. In terms of electrocatalysis, although various non-noble metal-based nanoparticles have been utilized, Pt and Ag containing nanoparticles outperform other systems. Therefore, there is a gap that can be filled by developing such non-noble metal-based nanoparticles, which can perform better than or at par with noble metal-based catalysts.

Conflicts of interest

There are no conflicts to declare.

Data availability

No primary research results, software or code have been generated as a part of this perspective.

Acknowledgements

A. T. acknowledges DST for the INSPIRE Fellowship [DST/INSPIRE Fellowship/2021/IF210531]. S. P. acknowledges DST for the INSPIRE Fellowship [DST/INSPIRE Fellowship/2021/IF210150]. A. K. acknowledges the support of DST under the PURSE scheme [file number: SR/PURSE/2023/199] and Anusandhan National Research Foundation (ANRF) for financial support under ANRF TARE (previously SERB TARE) with file number [TAR/2023/000169].

References

1 G. Pacchioni, *Nat. Mater.*, 2009, **8**, 167–168.
2 S. Malik, K. Muhammad and Y. Waheed, *Molecules*, 2023, **28**, 661.
3 T. Kumar, R. K. Pandey, R. Kumar, C. V. Sudheep, S. Sreelakshmi, S. Awasthi, Vandana and R. Singhal, Historical Perspective of Nanotechnology and Functionalized Nanomaterials, in *Functionalized Nanomaterials Based Supercapacitor: Design, Performance and Industrial Applications*, ed. C. M. Hussain and M. B. Ahamed, Springer Nature, Cham, 2023, pp. 1–24.
4 G. Liden, *Ann. Occup. Hyg.*, 2011, **55**, 1–5.
5 B. Zhou, R. Balee and R. Groenendaal, *Nanotechol. Law Bus.*, 2005, **2**, 222.
6 L. Jin, B. Liu, S. S. Duay and J. He, *Catalysts*, 2017, **7**, 44.
7 Z. Li, M. Li, Z. Bian, Y. Kathiraser and S. Kawi, *Appl. Catal., B*, 2016, **188**, 324–341.
8 C. T. Campbell, *Science*, 2004, **306**, 234–235.
9 M. Haruta, *Chem. Rec.*, 2003, **3**, 75–87.
10 Z. Ma and S. Dai, *Nano Res.*, 2011, **4**, 3–32.
11 S. A. C. Carabineiro, N. Bogdanchikova, M. Avalos-Borja, A. Pestryakov, P. B. Tavares and J. L. Figueiredo, *Nano Res.*, 2011, **4**, 180–193.
12 D. Astruc, F. Lu and J. R. Aranzaes, *Angew. Chem., Int. Ed.*, 2005, **44**, 7852–7872.
13 J. A. Widegren and R. G. Finke, *J. Mol. Catal. A: Chem.*, 2003, **198**, 317–341.
14 V. Polshettiwar and R. S. Varma, *Green Chem.*, 2010, **12**, 743–754.
15 K. N. L. Hoang, S. M. McClain, S. M. Meyer, C. A. Jalomo, N. B. Forney and C. J. Murphy, *Chem. Commun.*, 2022, **58**, 9728–9741.
16 K. An and G. A. Somorjai, *ChemCatChem*, 2012, **4**, 1512–1524.
17 G. A. Somorjai, H. Frei and J. Y. Park, *J. Am. Chem. Soc.*, 2009, **131**, 16589–16605.
18 J. A. Gladysz, *Pure Appl. Chem.*, 2001, **73**, 1319–1324.
19 A. Tyagi, N. Kunwar, S. Purohit, K. K. Pant and A. Kumar, *Polyhedron*, 2025, **277**, 117569.
20 A. Tyagi, S. Purohit, P. Oswal, V. Negi, S. Rawat, N. Bhatt, P. Sharma, A. K. Singh and A. Kumar, Sulphur donor containing Schiff base ligands in Homogeneous catalysis: Synthesis, Characterization and Applications, in *Homogeneous catalysis Concepts and Basics*, ed. M. R. Rahimpour, M. A. Makarem, T. Roostaei and M. Meshksar, Elsevier, Amsterdam, 2024, pp. 93–125.
21 E. Tobler, *Sulfur*, Enslow Publishing, New York, 2018.
22 L. Lu, S. Zou and B. Fang, *ACS Catal.*, 2021, **11**, 6020–6058.
23 A. Heuer-Jungemann, N. Feliu, I. Bakaimi, M. Hamaly, A. Alkilany, I. Chakraborty, A. Masood, M. F. Casula, A. Kostopoulou, E. Oh, K. Susumu, M. H. Stewart, I. L. Menditz, E. Statakis, W. J. Parak and A. G. Kanaras, *Chem. Rev.*, 2019, **119**, 4819–4880.
24 L. M. Rossi, L. L. Vono, M. A. Garcia, T. L. Faria and J. A. Lopez-Sanchez, *Top. Catal.*, 2013, **56**, 1228–1238.
25 R. D. Neal, R. A. Hughes, P. Sapkota, S. Ptasinska and S. Neretina, *ACS Catal.*, 2020, **10**, 10040–10050.
26 L. Lu, H. Zheng, Y. Li, Y. Zhou and B. Fang, *Chem. Eng. J.*, 2023, **451**, 138668.
27 A. Fihri, M. Bouhrara, B. Nekoueishahraki, J. M. Basset and V. Polshettiwar, *Chem. Soc. Rev.*, 2011, **40**, 5181–5203.
28 A. Roucoux, J. Schulz and H. Patin, *Chem. Rev.*, 2002, **102**, 3757–3778.
29 Y. A. Attia and S. H. Abdel-Hafez, *New J. Chem.*, 2018, **42**, 9606–9611.
30 M. Zdražil, *Catal. Today*, 1988, **3**, 269–365.
31 X. Li, A. Sotto, J. Li and B. V. D. Bruggen, *J. Membr. Sci.*, 2017, **524**, 502–528.

32 C. J. Huang, L. C. Wang, C. Y. Liu, A. S. Chiang and Y. C. Chang, *Biointerphases*, 2014, **9**, 029010.
33 K. Hiroi, Y. Suzuki, I. Abe, Y. Hasegawa and K. Suzuki, *Tetrahedron: Asymmetry*, 1998, **9**, 3797–3817.
34 D. Zaramella, P. Scrimin and L. J. Prins, *J. Am. Chem. Soc.*, 2012, **134**, 8396.
35 V. K. Jain, *Coord. Chem. Rev.*, 2021, **427**, 213546.
36 A. Arora, P. Oswal, G. K. Rao, J. Kaushal, S. Kumar, A. K. Singh and A. Kumar, *ChemistrySelect*, 2019, **4**, 10765.
37 P. Singh and A. K. Singh, *Dalton Trans.*, 2017, **46**, 10037–10049.
38 S. Gupta, N. Chandna, A. K. Singh and N. Jain, *J. Org. Chem.*, 2018, **83**, 3226–3235.
39 B. Chakraborty, S. Kalra, R. Beltrán-Suito, C. Das, T. Hellmann, P. W. Menezes and M. Driess, *Chem. – Asian J.*, 2020, **15**, 852–859.
40 C. Gervas, M. D. Khan, S. Mlowe, C. Zhang, C. Zhao, R. K. Gupta, M. P. Akerman, P. Mashazi, T. Nyokong and N. Revaprasadu, *ChemElectroChem*, 2019, **6**, 2560–2569.
41 G. E. Ayom, M. D. Khan, T. Ingsel, W. Lin, R. K. Gupta, S. J. Zamisa, W. E. Zyl and N. Revaprasadu, *Chem. – Eur. J.*, 2020, **26**, 2693–2704.
42 R. Akram, M. D. Khan, C. Zequine, C. Zhao, R. K. Gupta, M. Akhtar, J. Akhtar, M. A. Malik, N. Revaprasadu and M. H. Bhatti, *Mater. Sci. Semicond. Process.*, 2020, **109**, 104925.
43 C. Panda, P. W. Menezes, S. Yao, J. Schmidt, C. Walter, J. N. Hausmann and M. Driess, *J. Am. Chem. Soc.*, 2019, **141**, 13306–13310.
44 M. A. Agoro, J. Z. Mbese and E. L. Meyer, *Molecules*, 2020, **25**, 1919.
45 S. Khirid, R. Biswas, S. Meena, R. A. Patil, Y.-R. Ma, R. S. Devan, R. S. Dhayal and K. K. Haldar, *ChemistrySelect*, 2020, **5**, 10593–10598.
46 F. Saleem, G. K. Rao, A. Kumar, S. Kumar, M. P. Singh and A. K. Singh, *RSC Adv.*, 2014, **4**, 56102–56111.
47 S. Kumar, G. K. Rao, A. Kumar, M. P. Singh and A. K. Singh, *Dalton Trans.*, 2013, **42**, 16939–16948.
48 G. K. Rao, A. Kumar, F. Saleem, M. P. Singh, S. Kumar, B. Kumar, G. Mukherjee and A. K. Singh, *Dalton Trans.*, 2015, **44**, 6600–6612.
49 R. Bhaskar, A. K. Sharma, M. K. Yadav and A. K. Singh, *Dalton Trans.*, 2017, **46**, 15235–15248.
50 F. Ortloff, J. Bohnau, U. Kramar, F. Graf and T. Kolb, *Appl. Catal., B*, 2016, **182**, 550–561.
51 I. J. Ferrer, P. Diaz-Chao, A. Pascual and C. Sánchez, *Thin Solid Films*, 2007, **515**, 5783–5786.
52 W. Xu, J. Ni, Q. F. Zhang, F. Feng, Y. Z. Xiang and X. N. Li, *J. Mater. Chem. A*, 2013, **1**, 12811–12817.
53 Q. F. Zhang, W. Xu, X. N. Li, D. H. Jiang, Y. Z. Xiang, J. G. Wang, J. Cen, S. Romano and J. Ni, *Appl. Catal., A*, 2015, **497**, 17–21.
54 A. J. Mccue, A. Guerrero-Ruiz, I. Rodríguez-Ramos and J. A. Anderson, *J. Catal.*, 2016, **340**, 10–16.
55 F. Menegazzo, P. Canton, F. Pinna and N. Pernicone, *Catal. Commun.*, 2008, **9**, 2353–2356.
56 A. J. Mccue and J. A. Anderson, *Cheminform*, 2014, **4**, 272–294.
57 K. N. Sharma, H. Joshi, V. V. Singh, P. Singh and A. K. Singh, *Dalton Trans.*, 2013, **42**, 3908–3918.
58 F. Grønvold and E. Røst, *Acta Crystallogr.*, 1962, **15**, 11–13.
59 L. L. Long, A. Y. Zhang, Y. X. Huang, X. Zhang and H. Q. Yu, *J. Mater. Chem. A*, 2015, **3**, 4301–4306.
60 H. Fischmeister, *Acta Chem. Scand.*, 1959, **13**, 852–853.
61 B. D. Morreale, B. H. Howard, O. Iyoha, R. M. Enick, C. Ling and D. S. Sholl, *Ind. Eng. Chem. Res.*, 2007, **46**, 6313–6319.
62 C. P. O'Brien, A. J. Gellman, B. D. Morreale and J. B. Miller, *J. Membr. Sci.*, 2011, **371**, 263–267.
63 D. Albani, M. Shahrokhi, Z. Chen, S. Mitchell, R. Hauert, N. López and J. Pérez-Ramírez, *Nat. Commun.*, 2018, **9**, 2634.
64 W. Jing, S. Mo, W. Zhang, W. Zhou, K. Liu, J. Wei, R. Qin and N. Zheng, *Precis. Chem.*, 2024, **2**, 200–207.
65 V. V. Singh, U. Kumar, S. N. Tripathi and A. K. Singh, *Dalton Trans.*, 2014, **43**, 12555–12563.
66 W. Wang, D. Zhao, J. Yu, L. Shi, Y. Wang and H. Chen, *Nano Res.*, 2023, **16**, 2597–2603.
67 Y. Xu, K. Ren, T. Ren, M. Wang, S. Yu, Z. Wang, X. Li, L. Wang and H. Wang, *J. Mater. Chem. A*, 2020, **8**, 19873–19878.
68 L. Ma, S. Yuan, H. Zhu, T. Jiang, X. Zhu, C. Lu and X. Li, *Catalysts*, 2019, **9**, 410.
69 M. Bochmann, *Chem. Vap. Deposition*, 1996, **2**, 85–96.
70 V. K. Jain, *J. Chem. Sci.*, 2006, **118**, 547–552.
71 A. A. Tedstone, A. B. Jumah, E. Asuquo and A. A. Garforth, *R. Soc. Open Sci.*, 2022, **9**, 211353.
72 S. Shen, Y. Zhang, L. Peng, B. Xu, Y. Du, M. Deng, H. Xu and Q. Wang, *CrystEngComm*, 2011, **13**, 4572–4579.
73 P. Oswal, A. Arora, S. Singh, G. K. Rao, S. Kumar, A. K. Singh and A. Kumar, *Catal. Commun.*, 2021, **149**, 106242.
74 S. B. Somvanshi, S. R. Patade, D. D. Andhare, S. A. Jadhav, M. V. Khedkar, P. B. Kharat, P. P. Khirade and K. Jadhav, *J. Alloys Compd.*, 2020, **835**, 155422.
75 S. B. Somvanshi, S. A. Jadhav, M. V. Khedkar, P. B. Kharat, S. More and K. Jadhav, *Ceram. Int.*, 2020, **46**, 13170–13179.
76 S. B. Somvanshi, P. B. Kharat, T. S. Saraf, S. B. Somwanshi, S. B. Shejul and K. M. Jadhav, *Mater. Res. Innovations*, 2020, **25**, 169–174.
77 A. Bhosale, S. B. Somvanshi, V. Murumkar and K. Jadhav, *Ceram. Int.*, 2020, **46**, 15372–15378.
78 S. B. Somvanshi, P. B. Kharat, M. V. Khedkar and K. Jadhav, *Ceram. Int.*, 2020, **46**, 7642–7653.
79 S. B. Somvanshi, M. V. Khedkar, P. B. Kharat and K. Jadhav, *Ceram. Int.*, 2020, **46**, 8640–8650.
80 J. A. Darr, J. Zhang, N. M. Makwana and X. Weng, *Chem. Rev.*, 2017, **117**, 11125–11238.
81 Y. Guo, Z. Wang, H. Shao and X. Jiang, *Carbon*, 2013, **52**, 583–589.
82 M. Zhu, Y. Wang, D. Meng, X. Qin and G. Diao, *J. Phys. Chem. C*, 2012, **116**, 16276–16285.
83 A. K. Ganguli, T. Ahmad, S. Vaidya and J. Ahmed, *Pure Appl. Chem.*, 2008, **80**, 2451–2477.

84 M. López-Quintela, J. Rivas, M. Blanco and C. Tojo, Synthesis of nanoparticles in microemulsions, in *Nanoscale materials*, Springer, Berlin, 2004, pp. 135–155.
85 S. R. Patade, D. D. Andhare, S. B. Somvanshi, S. A. Jadhav, M. V. Khedkar and K. Jadhav, *Ceram. Int.*, 2020, **46**, 25576–25583.
86 P. B. Kharat, S. More, S. B. Somvanshi and K. Jadhav, *J. Mater. Sci.: Mater. Electron.*, 2019, **30**, 6564–6574.
87 S. B. Somvanshi, R. V. Kumar, J. S. Kounsalye, T. S. Saraf and K. Jadhav, *J. Phys.: Conf. Ser.*, 2020, **1644**, 012046.
88 A. R. Chavan, S. B. Somvanshi, P. P. Khirade and K. Jadhav, *RSC Adv.*, 2020, **10**, 25143–25154.
89 H. Kardile, S. B. Somvanshi, A. R. Chavan, A. Pandit and K. Jadhav, *Optik*, 2020, **207**, 164462.
90 C. Q. Sun, *Prog. Solid State Chem.*, 2007, **35**, 1–159.
91 L. Pan, M. Gu, G. Ouyang and C. Q. Sun, *Key Eng. Mater.*, 2010, **444**, 17–45.
92 R. Ouyang, J.-X. Liu and W.-X. Li, *J. Am. Chem. Soc.*, 2013, **135**, 1760.
93 F. Gambinossi, S. E. Mylon and J. K. Ferri, *Adv. Colloid Interface Sci.*, 2015, **222**, 332–349.
94 L. M. Rossi, J. L. Fiorio, M. A. S. Garcia and C. P. Ferraz, *Dalton Trans.*, 2018, **47**, 5889–5915.
95 P. Sharma, A. Arora, P. Oswal, G. K. Rao, J. Kaushal, S. Kumar, S. Kumar, M. P. Singh, A. K. Singh and A. Kumar, *Polyhedron*, 2019, **171**, 120–127.
96 P. Oswal, A. Arora, J. Kaushal, G. K. Rao, S. Kumar, A. K. Singh and A. Kumar, *RSC Adv.*, 2019, **9**, 22313–22319.
97 S. Kumar, G. K. Rao, A. Kumar, M. P. Singh, F. Saleem and A. K. Singh, *RSC Adv.*, 2015, **5**, 20081–20089.
98 K. Said, A. Mesni and R. B. Salem, *Lett. Org. Chem.*, 2020, **17**, 36–45.
99 P. Devendar, R.-Y. Qu, W.-M. Kang, B. He and G.-F. Yang, *J. Agric. Food Chem.*, 2018, **66**, 8914.
100 A. T. K. Koshvandi, M. M. Heravi and T. Momeni, *Appl. Organomet. Chem.*, 2018, **32**, e4210.
101 S. Jagtap, *Catalysts*, 2017, **7**, 267.
102 Y.-H. Ding, H.-X. Fan, J. Long, Q. Zhan and Y. Chen, *Bioorg. Med. Chem. Lett.*, 2013, **23**, 6087.
103 J. G. D. Vries, *Can. J. Chem.*, 2001, **79**, 1086.
104 P. Oswal, A. Arora, S. Gairola, A. Datta and A. Kumar, *New J. Chem.*, 2021, **45**, 21449–21487.
105 M. Karak, L. C. A. Barbosa and G. C. Hargaden, *RSC Adv.*, 2014, **4**, 53442.
106 K. Nejati, S. Ahmadi, M. Nikpassand, P. D. K. Nezhada and E. Vessally, *RSC Adv.*, 2018, **8**, 19125.
107 L. Lv and Z. Li, Fe-Catalyzed Cross-Dehydrogenative Coupling Reactions. Ni- and Fe-Based Cross-Coupling Reactions, in *Ni- and Fe- Based Cross-Coupling Reactions*, ed. A. Correa, Springer, Cham, 2016, pp. 225–263.
108 C. J. Li, *Acc. Chem. Res.*, 2009, **42**, 335–344.

